

Study of the Electronic Properties of a Fluoropyrazolecarbonitrile Derivative and Enhancement of Spectral Properties on Adsorption with Fullerene

Thangaiyan Pooventhiran^{1,2}, Korada Rajashekaraiah Shadakshara Murthy³, Rajimon Kalambukattu Joseph¹, Renjith Thomas^{1,*}

¹ Department of Chemistry, St Berchmans College (Autonomous), Mahatma Gandhi University, Changanassery, Kerala, 686101, India

² Department of Mechanical Engineering, University Centre for Research & Development Chandigarh University, Gharuan, Mohali, Punjab, India

³ Department of Chemical Engineering, Siddaganga Institute of Technology, Tumkur-572103, Karnataka, India

* Correspondence: renjith@scollege.ac.in (R.T.);

Scopus Author ID 55481779800

Received: 25.04.2022; Accepted: 5.06.2022; Published: 11.09.2022

Abstract: The molecule 5-amino-1-(2,6-dichloro-4-(trifluoromethyl)phenyl)-1H-pyrazole-3-carbonitrile is a pyrazole derivative with five different functional points. The main aim of this manuscript is to identify whether the compound interacts with fullerene molecules. The molecule's structure was simulated DFT- B3LYP/6-311+G (2d, p). The electronic spectra were generated using RCAM-B3LYP functional and the same basis sets with different solvents. Physical and chemical properties like active sites, biological activities, stabilities, solvation energy, electrons' occupancies in bonding orbitals, weak and strong hydrogen bonds, the steric force of interactions, delocalization of electrons, and reactive sites identification are reported. PASS and subsequent docking studies indicate the antiarthritic property. This molecule has good absorption energy (ΔH) -71.84 kcal/mol with a fullerene complex. Also, we found an enhancement of Raman activity of the compound when adsorbed with fullerene.

Keywords: carbonitrile; solvation effect; NBO; wavefunction; ALIE; MESP.

© 2021 by the authors. This article is an open-access article distributed under the terms and conditions of the Creative Commons Attribution (CC BY) license (<https://creativecommons.org/licenses/by/4.0/>).

1. Introduction

The derivatives of pyrazole are heterocyclic aromatic compounds partaking in medicinal and pesticide chemistry by their bioactivity [1]. The substituted pyrazoles are great-affinity ligands with estrogen receptor (E.R.) and have significantly great potential as an agonist on the ER α than on the ER β subtype [2]. Some pyrazoles have potential against human pathogens with high adaptivity against antimicrobial diseases ranging from soft tissue like bacteremia, endocarditis, pneumonia, and osteomyelitis, like *Staphylococcus aureus* [3], active against colorectal cancer cell lines HCT116 and SW620 [4], and clinical agent for the treatment of osteoporosis [5]. The derivatives of biphenyl pyrazole-benzofuran possess an inhibitory effect against α -glucosidase activity [6].

Curcumin pyrazole derivatives are active against Parkinson's disease. It is the deposition of neurotoxic α -synuclein aggregates in the brain during the development of neurodegenerative diseases and can be curbed by anti-aggregation strategies [7]. Derivatives of pyrazole carboxamide show antifungal activities against *Botrytis cinerea*, a necrotrophic

pathogenic fungus that causes significant crop loss in many plant species [8]. The substituents of strobilurin are the most important classes of agricultural fungicides [9]. Compounds like hymexazole, rabenzazole, and pyraclostrobin are fungicides derived from pyrazole, and these led to the commercial introduction of many industries [10].

The molecule 5-amino-1-(2,6-dichloro-4-(trifluoromethyl)phenyl)-1H-pyrazole-3-carbonitrile has three major functional groups acetonitrile, aminoimidazole, and chlorinated trifluoromethylphenyl. The multicomponent reactions (MCRs) are one of the best ways to synthesize heterocyclic compounds starting from simple and readily available materials [11]. Organic cyano compounds easily undergoes heterocyclation reactions by the addition of nucleophile to the cyano group [12], photoisomerization reaction [13], condensation reaction [14–16], cyclocondensation [17], addition reaction [18], reductive coupling reaction [19, 20], cross-coupling [21], substitution reaction [22, 23], and catalytic reactions [24].

The applications of acetonitrile, pyrazole and imidazole derivatives are biosynthesis of hemeproteins [14], anti-inflammatory [25], using photodynamic therapy for the treatment of cancer [15], anticancer activity [22, 26, 27], antiviral activity [1], anti-tuberculosis activity [28], control the activity of GPR139-protein in central nervous system [29], DNA labeling [30], polymerization/copolymerization [23], insecticidal activity [20], antifungal [10], Parkinson's disease [7], biogas energy [31] and battery energy [32].

In general, pyrazole derivatives contain C-N (especially lone pairs of nitrogen). They are used for their analgesic, antipyretic, anti-inflammatory (e.g., antipyrine, phenylbutazone, celecoxib), antibacterial, tranquilizing, anticancer, and antidiabetic activities [33, 34]. The molecule 5-amino-1-(2,6-dichloro-4-(trifluoromethyl)phenyl)-1H-pyrazole-3-carbonitrile is a famous insecticide [35].

In this paper, we report the theoretical investigations by DFT [36–38] calculations of structure, light-harvesting efficiency, solvent effects, nature of bonding orbitals, average localized ionization energy, electrostatic potentials, non-covalent interaction, and molecular docking assay of 5-amino-1-(2,6-dichloro-4-(trifluoromethyl)phenyl)-1H-pyrazole-3-carbonitrile. We also adsorbed the molecule with fullerene and found that there is effective adsorption and also, an enhancement in Raman activity of the system.

2. Materials and Methods

Optimization of carbonitrile done by Gaussian-09 [39] software, and package using the basis set of 6-311+G(2d,p) [40–44] with DFT- B3LYP [45–49] method. The ultraviolet-visible spectrum simulation calculation with TD-DFT using long-range corrected RCAM-B3LYP functional [50, 51] and 6-311G+(2d,p) method and basis set. We used to visualize the result and recover using from GaussSum [52] software. Reaction sites of carbonitrile were calculated using Multi-wavefunction software by analyzing wave functions like average localized ionization energy, total electrostatic potentials, and non-covalent interactions [53]. The structural relative bio-activity of carbonitrile was collected using PASS online webserver, high activity of corresponding PDB IDs downloaded from RCSB site [54], and the molecule docked with suitable protein using AutoDock_Vina [55], and docked results were visualized with the help of Discovery Studio [56] software.

3. Results and Discussion

3.1. Structure elucidation of carbonitrile.

Figure 1 shows the geometry of carbonitrile, and it poses 25 atoms with the contributions of three fluorine, two chlorine, four nitrogen, 11 carbon, and five hydrogen atoms. The prominently bond lengths of C-F in the trifluoromethan- group between 1.30 and 1.36 Å, C-N in 1^0 amines, and pyrazole between 1.37 and 1.50 Å, C-C near 1.50 Å, C-N in nitril- is 1.16 Å, and C-Cl between 1.73 and 1.75 Å: bond angles of C9 in trifluoromethyl between 1.07 and 111.56 0 , N19 and N20 in pyrazole and 1^0 amines between 103.50 and 127.80 0 .

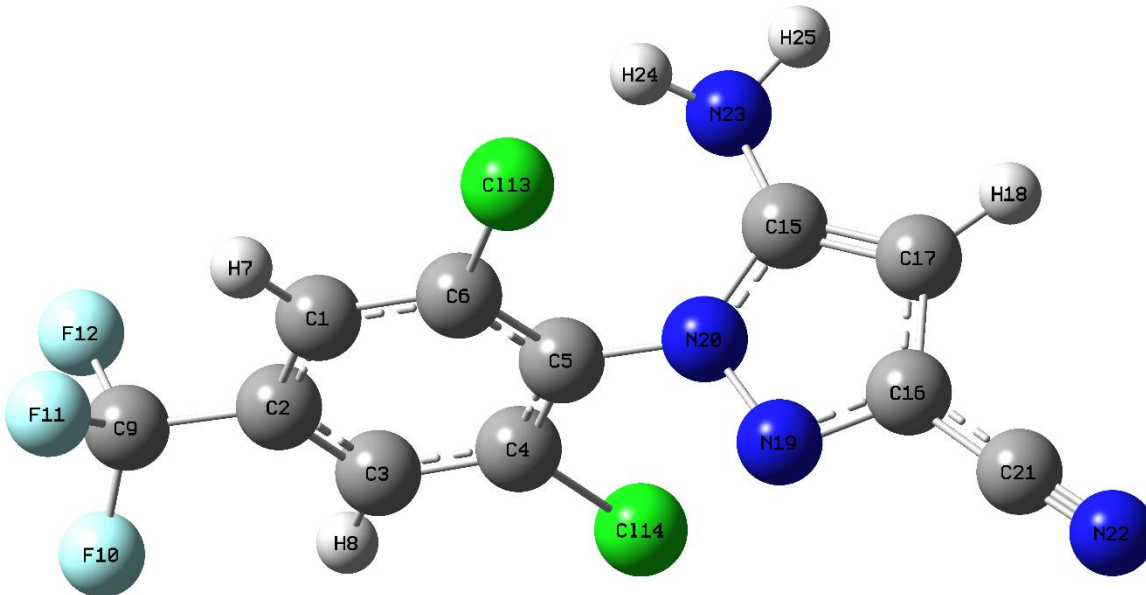


Figure 1. Optimized geometry of carbonitrile.

3.2. Light-harvesting efficiency (LHE), and free solvent energy (ΔG^0) of carbonitrile.

The energy calculation of the electronic transition study done by TD-DFT utilizing RCAM-B3LYP/6-311+G(2d,p) with carbonitrile with the polar and nonpolar solvents like water, ethanol, and dimethylsulfoxide (DMSO) implicit solvents atmosphere IEFPCM solvation model. The U.V.–Vis spectrum is given in Figure 2. The L.H.) and solvent energy of carbonitrile are shown in Table 1.

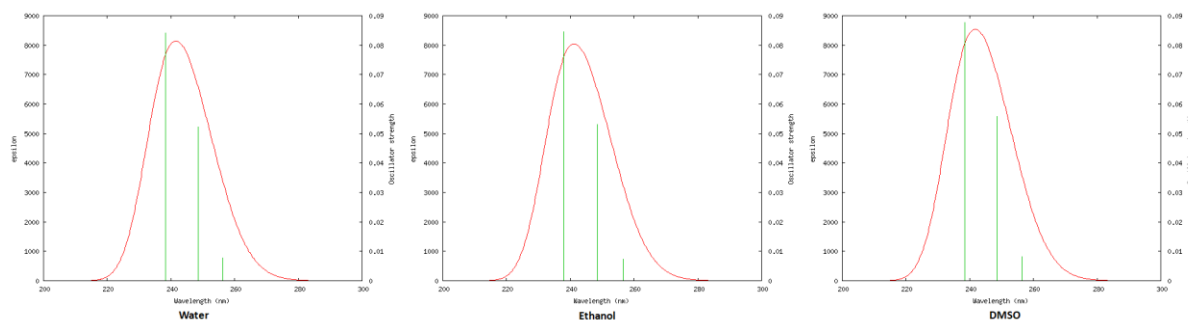


Figure 2. Electronic spectra of carbonitrile with solvents.

Table 1. LHE and free solvation energies of carbonitrile.

Solvents	Wavelength (nm)	Absorbance factor (f)	Light harvesting energy LHE=1-10 ^{-f}	Solvation energy ΔG ⁰ (in kcal/mol)
			in %	
Water	238.32	0.0842	0.1762	17.62 -2.2245
Ethanol	237.92	0.0845	0.1768	17.68 -2.7347
DMSO	238.41	0.0877	0.1871	18.71 -2.1360

The light-harvesting efficiency measures the fraction of light intensity absorbed by the dye. Here, we have done a theoretical investigation of this carbonitrile-derived molecule.

Carbonitrile is a polar molecule, so we selected polar solvents like water, ethanol, and DMSO. Carbonitrile dissolved into different solvents, water, ethanol, and DMSO, shows intensities at 238.32, 237.92, and 238.41 nm, and absorption factors (f) 0.0842, 0.0845 and 0.0877, respectively. The efficiency of carbonitrile can be calculated in theoretically as LHE [57–64], expressed as a function of the oscillator strength related as LHE=1-10^{-f} [65–67]. Carbonitrile having light-harvesting efficiency with solvents water, ethanol and DMSO are 0.1762, 0.1768, and 0.1828, and in percentage 17.62, 17.68, and 18.28, respectively. From the above result, carbonitrile does not have good light-harvesting efficiency due to poor percentages of capacity with selected solvents [68, 69].

Water and ethanol are polar solvents, and DMSO is an aprotic solvent. Carbonitrile showed red shifts and hypsochromic shifts due to higher intensities occurring at lower wavelengths (below 240 nm). Carbonitrile in water, ethanol, and DMSO shows free salvation energies (ΔG^0) are -2.2245 and -2.7347, and -2.1360 kcal/mol, respectively. These solvents can make dissolution with carbonitrile with a number of hydrogen bonds with water and ethanol, hydrogen bonds, and proton transfer interactions with DMSO. Solvent water produces a number of hydrogen bonds by oxygens with hydrogens in carbonitrile and halogens in carbonitrile with hydrogens in water, but solvent ethanol has a number of hydrogens than water and forms a greater number of hydrogen bonds than solvent water, and solvent DMSO makes hydrogen bonds between carbonitrile and DMSO through only donates of protons. From the above result, ethanol is a good solvent comparing selected polar solvents, with good solvation energy.

3.3. Adsorption (ΔH) assay of carbonitrile with fullerene-24.

The attractions between hydrogen and more electronegativity elements produce electrostatic effects between them [70–73]. The absorption property is found by frequency calculations of carbonitrile and fullerene (C24), and both of them shows in Figure 3 and Table 2.

The absorbance occurs between carbonitrile and fullerene with hydrogen bond attractions of halogens, nitrogen, and hydrogens. This assay is explained by increased complex intensity (carbonitrile with fullerene) compared with the individual intensities of carbonitrile and fullerene. Frequencies at 522.4, 556.90, 815.60, 1339.60, 1540.70, 1616.70, 1696.70, 2359.70, and 3527.90-3629.60 cm⁻¹ notable absorbances of C-F in phenyl- ring, C-H in fullerene ring, C-Cl in phenyl- ring, C-CF₃ in phenyl- ring, C-N is an aromatic bond in imidazol- ring, C=C of imidazol- ring, C-NH₂ in imidazole group, -C.N. is nitrile in imidazol-group, and N-H amine in imidazol- group respectively.

Absorption analysis also gives a change in enthalpy (ΔH) between reactants and products of making complex, which is the difference between the enthalpy of complex and individual of carbonitrile and fullerene:

$$\square H_{absorption} = H_{products} - H_{reactants}$$

$$\square H_{absorption} = H_{complex} - [H_{carbonitrile} + H_{fullerene}]$$

The enthalpies of carbonitrile, fullerene, and complex are -1860.8855, -913.6917, and -2774.5768 Hartree, respectively. Therefore, the change in enthalpy of the complex has -0.1145 Hartree, which is equal to -71.8499 kcal/mol.

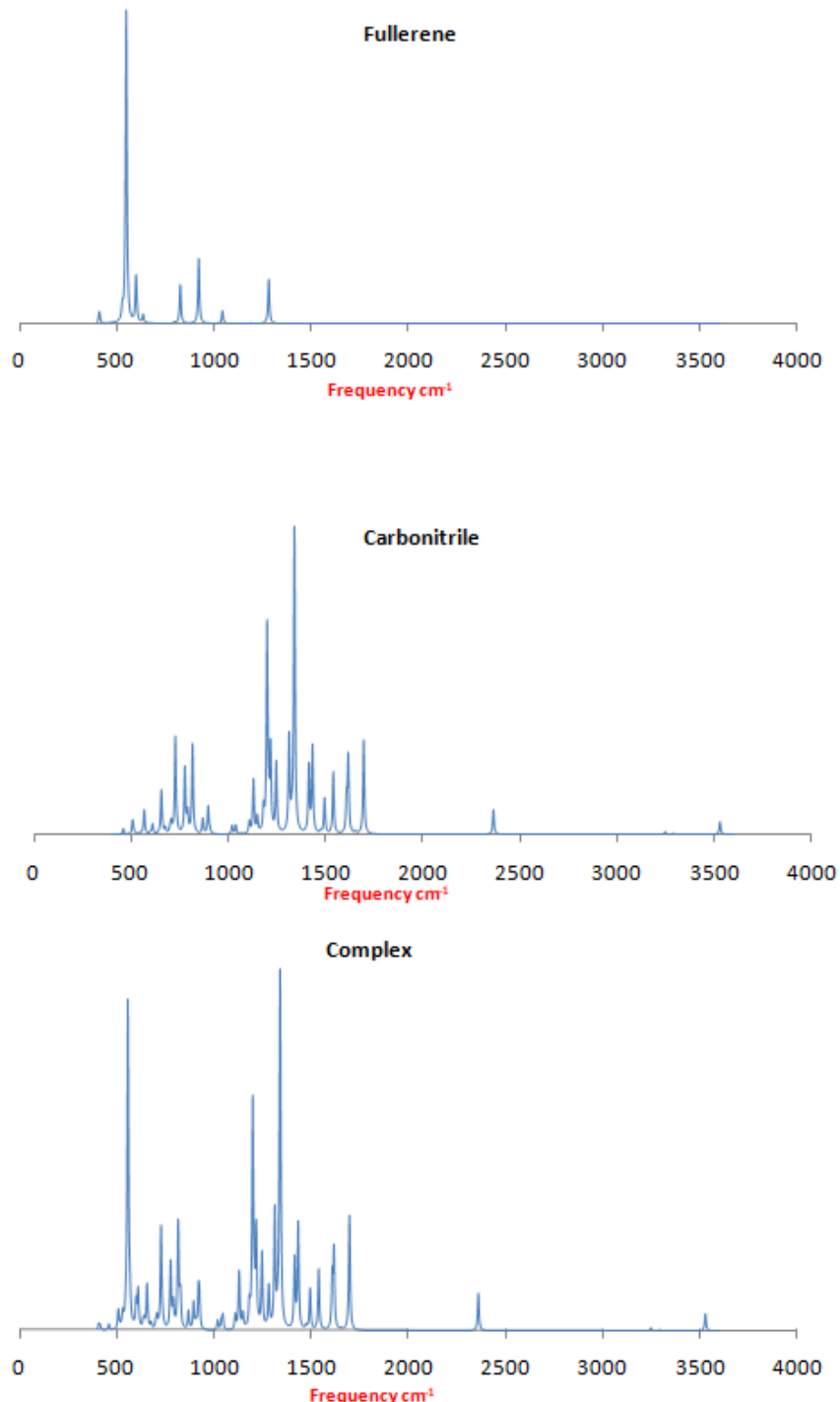


Figure 3. Absorption of carbonitrile on fullerene showing enhancement of spectral behavior.

Table 2. Absorbance of complexes of carbonitrile with fullerene.

Functional groups	Frequency (cm ⁻¹)	Absorbance		
		Complex	Carbonitrile	Fullerene
C-F (phenyl)	522.40	35.0812	9.73887	37.0356
C-H (fullerene)	556.90	1143.82	14.6884	210.305
C-Cl (phenyl)	815.60	385.45	352.558	15.227

Functional groups	Frequency (cm⁻¹)	Absorbance		
		Complex	Carbonitrile	Fullerene
C-CF ₃ (phenyl)	1339.60	1247.14	1193.26	0.73613
C-N (aromatic in imidazole)	1540.70	166.082	231.215	0.01636
C=C (imidazole)	1616.70	299.129	317.97	0.00013
C-NH ₂ (imidazole)	1696.70	398.501	360.191	0
-CN (nitrile in imidazole)	2359.70	129.627	52.6592	0
N-H (NH ₂)	3527.90-3629.60	58.9407-81.2998	46.3397 - 76.9548	0

3.4. Natural bonding orbital (NBO) assay.

Molecular structure and stability of carbonitrile are explained by NBO assay. Carbonitrile has 25 atoms (chlorine, fluorine, nitrogen, carbon, and hydrogen), which possess 586 atomic orbitals, angular momentums, types, occupancies of electrons, and energies (orbital) shown in **Table S1**. The valence orbital with 3pz (angular momentum) of chlorine atoms labeled as 13 and 14 shows 1.91 and 1.89 (near 2) occupancies, and energies are -0.36 and -0.35 a.u. respectively (in phenyl- ring); alike, valence orbital with 2pz (angular momentum) of fluorine atoms label as 10, 11 and 12 shows 1.89, 1.82 and 1.67 (near 2) occupancies, and energies are -0.47, -0.47 and -0.48 a.u. respectively (in phenyl- ring).

In the same way, the valence orbital with 2pz (angular momentum) of nitrogen atoms labeled as 19, 20, 22 and 23 shows 1.38, 1.24, 1.21 and 1.33 (near 1) occupancies, respectively, and energies are -0.21 a.u. (in imidazol- ring), -0.29 a.u. (in imidazol- ring), -0.16 a.u. (in acetonitril-) and -0.26 a.u. (amino-) respectively; valence orbital with 2pz (angular momentum) of carbon atoms has occupancies between 0.60 and 1.08 (near 1) and energy between -0.07 and -0.12 a.u.; similarly, the valence orbital with 1s (angular momentum) of hydrogen atoms have occupancies between 0.61 and 0.75 (near 1) and energy between 0.01 and 0.02 a.u. From the above result, all the valence electrons in carbonitrile are delocalized.

Table 3 displays the transition energies of carbonitrile from donor to acceptor orbitals. The electron transitions occur from donor bonding and antibonding orbitals of σ(2)C1-C2, σ(2)C1-C2, σ(2)C3-C4, σ(2)C3-C4, σ(2)C15-C17, L.P. (1)N20, L.P. (1)N20, L.P. (1)N22, L.P. (1)N23, σ*(2)C5-C6, σ*(2)C5-C6, σ*(2)C16-N19, and σ*(2)C16-N19 to acceptor antibonding orbitals of σ*(2)C3-C4, σ*(2)C5-C6, σ*(2)C1-C2, σ*(2)C5-C6, σ*(2)C16-N19, σ*(2)C15-C17, σ*(2)C16-N19, R*(1)C21, σ*(2)C15-C17, σ*(2)C1-C2, σ*(2)C3-C4, σ*(2)C15-C17, and σ*(3)C21-N22 using the amount of energies are 21.09, 21.18, 20.72, 21.50, 30.57, 41.47, 26.26, 18.48, 26.55, 174.87, 329.43, 125.44, and 22.12 kcal//mol respectively [74–76].

Table 3. Transition energies of carbonitrile.

NAOs	Donor NAO (i)	NAOs	Acceptor NAO (j)	E(2) kcal/mol	E(j)-E(i) a.u.	F(i,j) a.u.
2	σ(2) C1-C2	561	σ*(2) C3-C4	21.09	0.28	0.07
2	σ(2) C1-C2	566	σ*(2) C5-C6	21.18	0.27	0.07
8	σ(2) C3-C4	555	σ*(2) C1-C2	20.72	0.29	0.07
8	σ(2) C3-C 4	566	σ*(2) C5-C6	21.50	0.27	0.07
20	σ(2) C15-C17	578	σ*(2) C16-N19	30.57	0.27	0.09
78	LP(1) N20	573	σ*(2) C15-C17	41.47	0.3	0.10
78	LP(1) N20	578	σ*(2) C16-N19	26.26	0.28	0.08
79	LP(1) N22	478	R*(1) C21	18.48	1.62	0.16
80	LP(1) N23	573	σ*(2) C15-C17	26.55	0.34	0.09
566	σ*(2) C5-C6	555	σ*(2) C1-C2	174.87	0.02	0.08
566	σ*(2) C5-C6	561	σ*(2) C3-C4	329.43	0.01	0.08
578	σ*(2) C16-N19	573	σ*(2) C15-C17	125.44	0.02	0.06
578	σ*(2) C16-N19	584	σ*(3) C21-N22	22.12	0.12	0.09

3.5. Average localized ionization energy (ALIE) assay.

ALIE assay explains the stability of carbonitrile by nature of localized and delocalized electrons in the molecule. Figure 4 displays the nature of electrons. Carbonitrile has a length unit between -12.14 and 12.14 Bohr³, with the scale range from 0.00 to 2.00, denoting colors from blue to red. The delocalized electrons produce several carbonitrile resonance structures, which explains its stability.

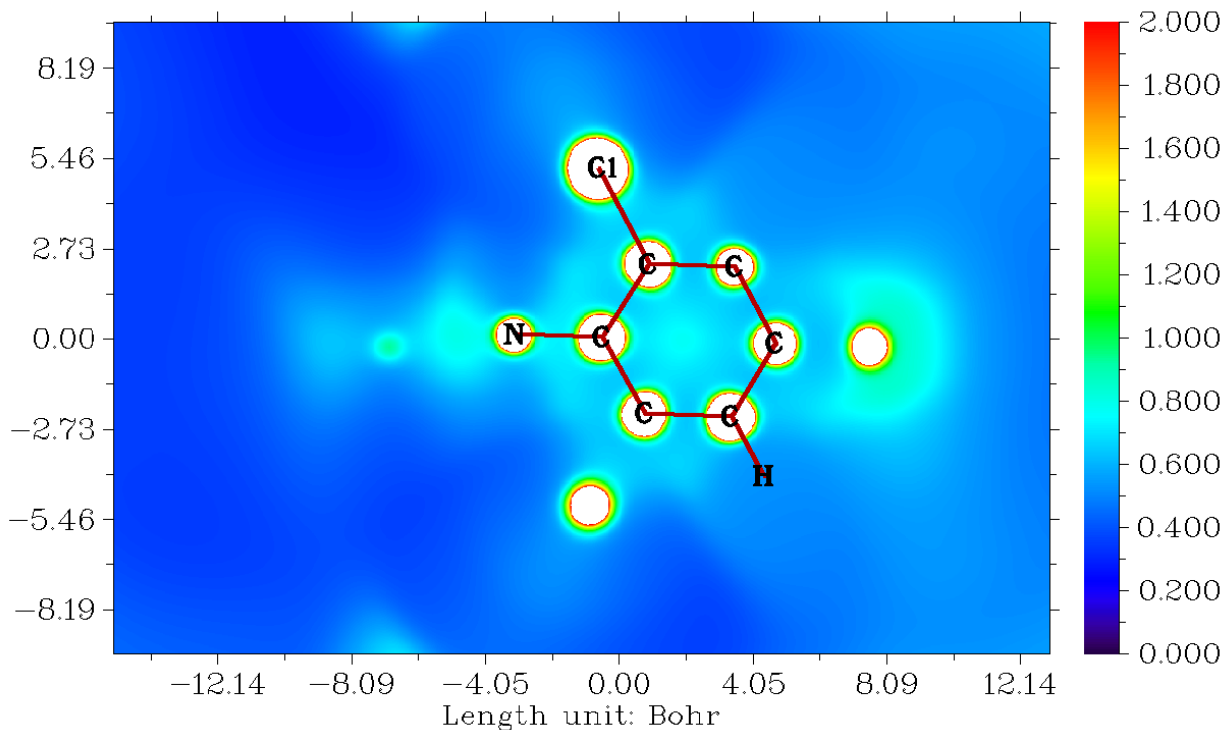


Figure 4. Average localized ionization energy of carbonitrile.

Color blue range between 0.20 and 0.50, mentioning that localized electrons of all hydrogen atoms and lone pairs of electrons contain all nitrogen atoms in carbonitrile. Similarly, a bluish-green color range between 0.70 and 1.20 mentions the delocalized electrons of chlorine-, fluorine-, carbon atoms in 1,3-dichloro-5-(trifluoromethyl)phenyl- and their pi system, and nitrogens and carbons in amino-, acetonitrile- and imidazole- and their pi system. Similarly, the red color range between 1.80 and 2.00 mentions those core electrons of heavy atoms like chlorine, fluorine, nitrogen, and carbon atoms in the whole molecule [71, 72].

3.6. Molecular electrostatic potentials (MESP) assay.

MESP explains the reactivity of carbonitrile by electrical and nuclear charges, which means these charges show active sites of electrophiles and nucleophiles. Figure 5 displays the electrical and nuclear charges of carbonitrile [77, 78].

MESP by electrical charges of carbonitrile represented by the length unit between -12.08 and 12.08 Bohr³, and scale from -0.10 to 0.10 by the color from blue to red. The blue color from -0.04 to -0.02 shows electron-rich sites of carbonitrile, which means lone pairs of electrons in all nitrogen atoms. Therefore, electrophiles attack (electrophilic reactions possible) these sites. The red color from 0.06 to 0.10 shows electron-poor sites of carbonitrile, which means carbon atoms that possess hydrogen atoms. Therefore, nucleophiles attack (nucleophilic reactions) these sites.

MESP by nuclear charges of carbonitrile represented by the length unit between -12.14 and 12.14 Bohr³, and scale from 0.00 to 50.00 by the color from blue to red. Carbonitrile having negative electrostatic potentials show high electron density shows large attractions of protons with nuclei due to the core and lone pair of electrons in heavy atoms are carbons, nitrogens, fluorines, and chlorines in the molecule at the nuclear charge between 47.00 and 50.00, and the positive electrostatic potentials show large repulsions of protons with nuclei due to no neutrons, core, and lone pair of electrons in all the hydrogen atoms in the molecule at nuclear charges between 17.00 and 23.00 have.

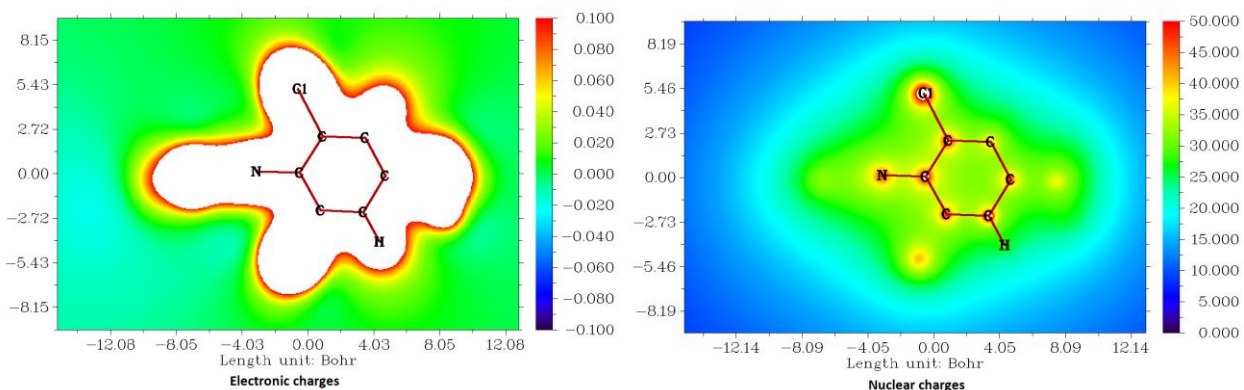


Figure 5. Molecular electrostatic potentials of carbonitrile.

3.7. Non-covalent interactions (NCI) assay.

NCI explains reactivity, especially biological activity based on hydrogen bonds of carbonitrile. Figure 6 represented hydrogen bond interactions of (strong, weak, and repulsion forces of) hydrogen bonds by a graph plotted energy against the reduced density gradient of carbonitrile [79–83].

Carbonitrile has energy from -0.15×10^{-1} to -0.05×10^{-1} a.u. show strong hydrogen bonds between nitrogen and hydrogen atoms of amino- in imidazole- group, alike energy from -0.05×10^{-1} to 0.04×10^{-1} a.u. shows van der Waals forces between chlorine and hydrogen atoms in 1,3-dichloro-5-(trifluoromethyl)phenyl- group, and energy from 0.06 to 0.24×10^{-1} a.u. shows hydrogens and pi repulsions between carbonitrileimidazol- and 1,3-dichloro-5-(trifluoromethyl)phenyl- groups. Also, in Figure 6, we represent the NCI between the fullerene and the molecule also. It is clear that there are enhanced weak interactions between fullerene and carbonitrile, which is evident from more green points in the scatter graph.

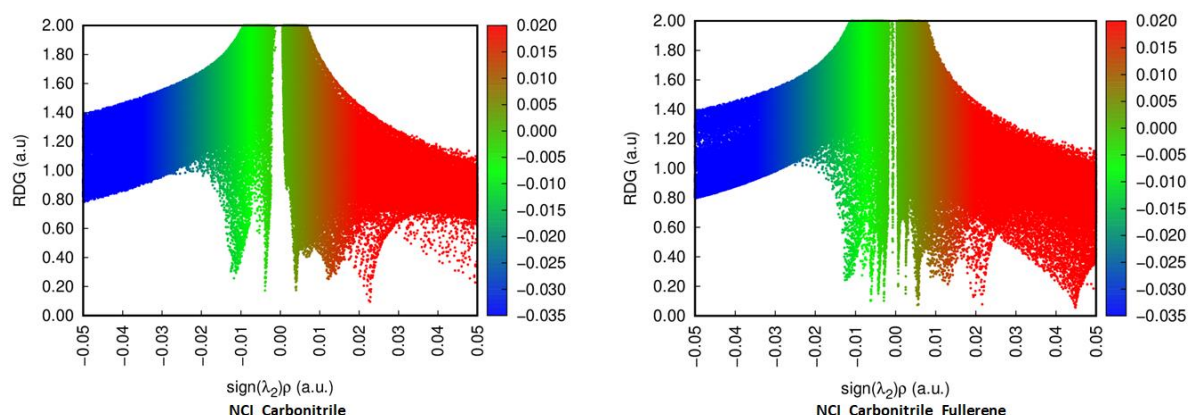


Figure 6. Non-covalent interactions of carbonitrile.

3.8. Molecular docking assay.

Table 4 shows the quantitatively structure-relative activity (QSRA) of carbonitrile predicted using the PASS online server, and the PASS result shows biological activity by probability to be active (0.63) and inactive (0.03) of carbonitrile having antiarthritic activity more than 50 percent. Structurally, carbonitrile is active against T cell receptor beta chains related to rheumatoid arthritis (R.A.). Therefore, the human immune system rheumatoid arthritis protein (PDB ID: 2AXJ) [84], was downloaded and did dock. This protein structure is derived from synovial fluid (SF4) and tissue (C5-1) of a patient with R.A.

Table 4. PASS-QSRA analysis of carbonitrile.

Pa	Pi	Activity
0.63	0.03	Antiarthritic
0.59	0.02	HMGCS2 expression enhancer
0.54	0.02	Neurodegenerative diseases treatment
0.49	0.02	Antiobesity
0.48	0.02	Protein kinase inhibitor
0.46	0.01	Interleukin antagonist
0.45	0.02	Antiparkinsonian
0.42	0.01	MAP kinase inhibitor
0.42	0.01	Dihydroorotate inhibitor
0.40	0.00	Potassium channel (Ca-activated) activator
0.38	0.02	Transplant rejection treatment
0.41	0.05	Autoimmune disorders treatment
0.37	0.03	CYP2C9 inhibitor
0.43	0.10	Complement factor D inhibitor

Pa - probability to be active; Pi - probability of being inactive.

Table 5 displays the binding affinity of carbonitrile and ibuprofen (as reference drug), and having -5.70 and -5.1 kcal/mol at zero root mean square deviation (rmsd) of both upper and lower bases, respectively. Table 6 shows five residues (list) of the protein that interact with carbonitrile and reference molecules (of side chain A), and Figure 7 displays the skeletal and 2D structure of interactions between carbonitrile, reference molecules, and protein.

Table 5. Binding affinity of carbonitrile.

Mode	Binding Affinity (kcal/mol)	Distance from best mode (Å)		Mode	Binding Affinity (kcal/mol)	Distance from best mode (Å)	
		rmsd low base	rmsd upper base			rmsd low base	rmsd upper base
Carbonitrile							
1	-5.70	0.00	0.00	1	-5.10	0.00	0.00
2	-5.70	0.31	2.16	2	-4.90	1.75	2.51
3	-5.70	1.13	1.96	3	-4.90	1.74	2.88
4	-5.60	1.09	2.81	4	-4.90	22.92	24.11
5	-5.50	4.42	6.20	5	-4.90	9.70	11.86
6	-5.50	6.06	8.16	6	-4.80	1.89	3.31
7	-5.50	6.07	8.23	7	-4.80	3.31	6.19
8	-5.50	4.38	6.48	8	-4.70	21.12	22.10
9	-5.40	17.03	18.12	9	-4.70	42.67	44.30

Table 6. Name and label of protein (PDB ID: 2AXJ) residues binding with carbonitrile and ibuprofen (as reference).

Compounds	Label of Protein Residues
Carbonitrile	ASP:3, ILE:6. LEU:103, PHE:104, and PHE:105
Ibuprofen	ARG 15, GLU 17, GLY 18, GLN 84, and VAL 113

ARG-arginine; ASP-aspartic acid; GLN-glutamine; GLU-glutamic acid; GLY-glycine; ILE-isoleucine; LEU-leucine; PHE-phenylalanine; and VAL-valine.

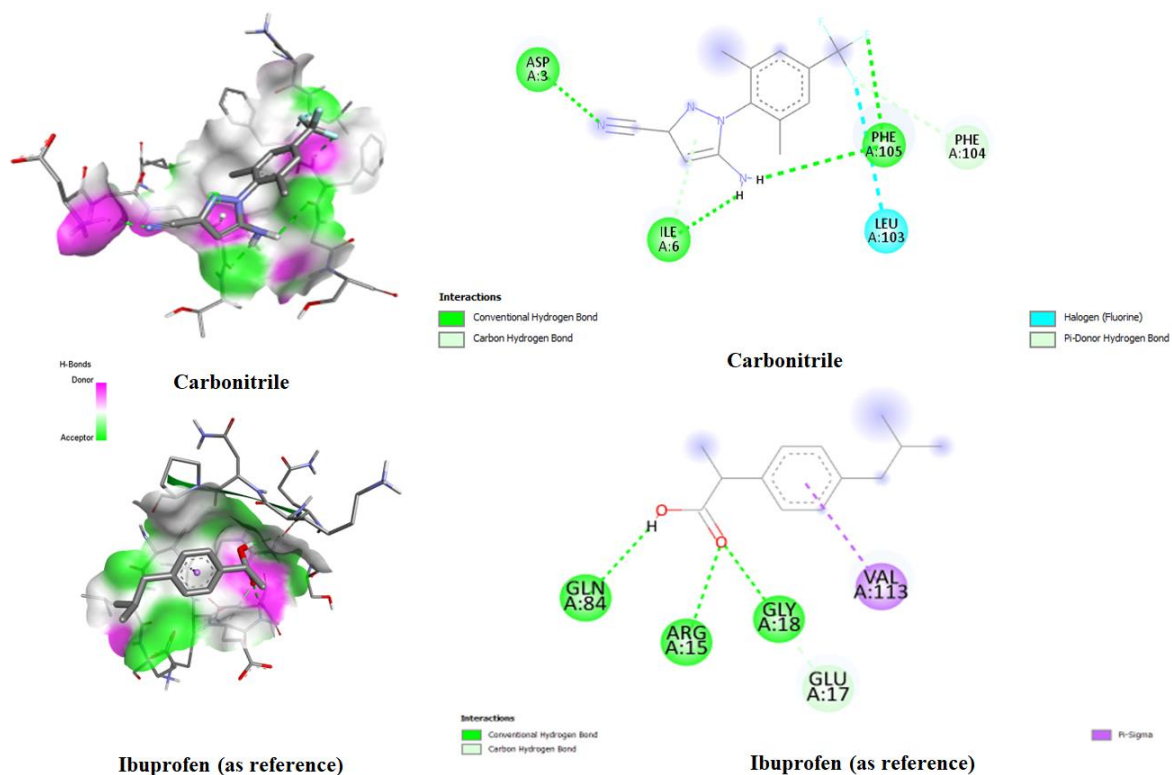


Figure 7. Skeletal and 2D structure of carbonitrile with protein.

Table S2 shows non-bond (including favourable and unsatisfied sites) interactions of carbonitrile in detail (including types and categories). Carbonitrile has four conventional hydrogen bonds as donors (hydrogen) from A:ASP3:HT2, A:PHE105:HN, :UNK0:H and :UNK0:H to acceptors (nitrogen, fluorine, and oxygen) :UNK0:N, :UNK0:F, A:PHE105:O and A:ILE6:O and the bond distances are 2.10, 2.32, 3.03 and 2.10 Å respectively. One carbon-hydrogen bond as a donor (hydrogen) from A:PHE104:CA to an acceptor (fluorine) :UNK0:F by the distance 3.27 Å, alike one pi-donor hydrogen bond donor (hydrogen) from A:ILE6:HN to acceptor pi orbital in :UNK0 with 3.00 Å, One halogen bond from halogen acceptor (oxygen) of A:LEU103:O to a halogen of :UNK0:F by the distance 3.52 Å. carbonitrile having one unsatisfied site is nitrogen as donor and details mentioned in Table S2 [85–89]. Similarly, the reference molecule has three conventional hydrogen bonds, one carbon-hydrogen bond, and one pi-sigma bond type of interaction with referred protein. Carbonitrile has a greater number of interactions and higher binding affinity than reference drugs.

4. Conclusions

From the result of the solvent effect, 5-amino-1-(2,6-dichloro-4-(trifluoromethyl)phenyl)-1H-pyrazole-3-carbonitrile shows a good effect with ethanol than water and DMSO, from NBO studies revealed the intensity of various intramolecular interactions and stability explained by the occupancies of electrons in orbitals and transition energies, from ALIE study shown the nature of localized electrons, from MESP study, explained the electrostatic potentials by electronic and nuclear charges, from NCI study discussed the non-covalent interactions of weak and strong hydrogen bonds and steric type of bond attractions. The structure relative activity is confirmed from PASS and binding affinity. This molecule has good absorption energy (ΔH) -71.8499 kcal/mol with a fullerene complex.

Funding

RT thanks the Royal Society of Chemistry, London, for support through the Research Fund grant with number R21-6353238377.

Acknowledgments

SEAGrid (<http://www.seagrid.org>) is acknowledged for computational resources and services for the selected results used in this publication.

Conflicts of Interest

The authors declare no conflict of interest.

References

1. Ouyang, G.; Cai, X.-J.; Chen, Z.; Song, B.-A.; Bhadury, P.S.; Yang, S.; Jin, L.-H.; Xue, W.; Hu, D.-Y.; Zeng, S. Synthesis and Antiviral Activities of Pyrazole Derivatives Containing an Oxime Moiety. *J. Agric. Food Chem.* **2008**, *56*, 10160–10167, <https://doi.org/10.1021/jf802489e>.
2. Stauffer, S.R.; Coletta, C.J.; Tedesco, R.; Nishiguchi, G.; Carlson, K.; Sun, J.; Katzenellenbogen, B.S.; Katzenellenbogen, J.A. Pyrazole Ligands: Structure - Affinity/Activity Relationships and Estrogen Receptor-. *J. Med. Chem.* **2000**, *43*, 4934–4947, <https://doi.org/10.1021/jm000170m>.
3. Johnston, T.; Ty, D. Van; Chen, R.F.; Fawzi, N.L.; Kwon, B.; Kelso, M.J.; Gilmore, M.S.; Mylonakis, E. Propyl-5-hydroxy-3-methyl- 1-phenyl-1 H -pyrazole-4- carbodithioate (HMPC): a new bacteriostatic agent against methicillin — resistant *Staphylococcus aureus*. *Sci. Rep.* **2018**, *8*, 7062, <https://doi.org/10.1038/s41598-018-25571-w>.
4. Xu, J.; Tan, H.; Zhang, Y.; Tang, D.; Zhan, F.; Li, H.; Chen, Z.-Z.; Xu, Z.-G. Catalyst-Free One-Pot Synthesis of Densely Substituted Pyrazole- Pyrazines as Anti-Colorectal Cancer Agents. *Sci. Rep.* **2020**, *10*, 9281, <https://doi.org/10.1038/s41598-020-66137-z>.
5. Joo, J.H.; Huh, J.; Lee, J.H. et al. A novel pyrazole derivative protects from ovariotomy-induced osteoporosis through the inhibition of NADPH oxidase. *Sci. Rep.* **2016**, *6*, 22389, <https://doi.org/10.1038/srep22389>.
6. Azimi, F.; Azizian, H.; Najafi, M. et al. Design , synthesis , biological evaluation , and molecular modeling studies of pyrazole - benzofuran hybrids as new α - glucosidase inhibitor. *Sci. Rep.* **2021**, *11*, 20776, <https://doi.org/10.1038/s41598-021-99899-1>.
7. Ahsan, N.; Mishra, S.; Jain, M.K.; Surolia, A.; Gupta, S. Curcumin Pyrazole and its derivative (N-(3-Nitrophenylpyrazole) Curcumin inhibit aggregation, disrupt fibrils and modulate toxicity of Wild type and Mutant a-Synuclei. *Sci. Rep.* **2015**, *5*, 9862, <https://doi.org/10.1038/srep09862>.
8. Xia, D.; Cheng, X.; Liu, X.; Zhang, C.; Wang, Y.; Liu, Q.; Zeng, Q.; Huang, N.; Cheng, Y.; Lv, X. Discovery of Novel Pyrazole Carboxylate Derivatives Containing Thiazole as Potential Fungicides. *J. Agric. Food Chem.* **2021**, *69*, 8358–8365, <https://doi.org/10.1021/acs.jafc.1c01189>.
9. Li, M.; Liu, C.-L.; Yang, J.-C.; Zhang, J.-B.; Li, Z.-N.; Zhang, H.; Li, Z.-M. Synthesis and Biological Activity of New (E)- α -(Methoxyimino)benzeneacetate Derivatives Containing a Substituted Pyrazole Ring. *J. Agric. Food Chem.* **2010**, *58*, 2664–2667, <https://doi.org/10.1021/jf9026348>.
10. Vicentini, C.B.; Romagnoli, C.; Andreotti, E.; Mares, D. Synthetic Pyrazole Derivatives as Growth Inhibitors of Some Phytopathogenic Fungi. *J. Agric. Food Chem.* **2007**, *55*, 10331–10338, <https://doi.org/10.1021/jf072077d>.
11. Kamalzare, M.; Aghhari, M.R.; Bayat, M.; Maleki, A. Fe₃O₄ @ chitosan - tannic acid bionanocomposite as a novel nanocatalyst for the synthesis of pyranopyrazoles. *Sci. Rep.* **2021**, *11*, 20021, <https://doi.org/10.1038/s41598-021-99121-2>.

12. Attanasi, O.A.; Santeusanio, S.; Serra-Zanetti, F.; Foresti, E.; McKillop, A. Conjugated azoalkenes. Part 8. Reaction of some conjugated azoalkenes with activated nitriles. Synthesis of new pyrrolo[2,3-*b*]pyrroles and 1,2-diaminopyrroles. X-Ray molecular structure of diethyl 6-amino-1,6-bis-(t-butoxycarbonylamino)-3a-cyano-2,5-dimethyl-1,3a,6,6a-tetrahydropyrrolo-[2,3-*b*]pyrrole-3,4-dicarboxylate. *J. Chem. Soc., Perkin Trans. I* **1990**, 1669-1675.
13. Behrens, S.; Jug, K. SINDO1 Study of the Photoisomerization of 2-Cyanopyrrole to 3-Cyanopyrrole. *J. Org. Chem.* **1990**, *55*, 2288–2294, <https://doi.org/10.1021/jo00295a011>.
14. Adamczyk, M.; Reddy, R.E. A convenient synthesis of 2-yanopyrroles from isocyanoacetonitrile. *Tetrahedron Lett.* **1995**, *36*, 7983–7986, [https://doi.org/10.1016/0040-4039\(95\)01724-V](https://doi.org/10.1016/0040-4039(95)01724-V).
15. Adamczyk, M.; Reddy, R.E. A new methodology for the preparation of 2-cyanopyrrholes and synthesis of porphobilinogen. *Tetrahedron* **1996**, *52*, 14689–14700, [https://doi.org/10.1016/0040-4020\(96\)00941-6](https://doi.org/10.1016/0040-4020(96)00941-6).
16. Araki, S.; Tanaka, T.; Toumatsu, S.; Hirashita, T. A new synthesis of pyrroles by the condensation of cyclopropenes and nitriles mediated by gallium(III) and indium(III) salts. *Org. Biomol. Chem.* **2003**, *1*, 4025–4029, <https://doi.org/10.1039/B308875H>.
17. Vilches-Herrera, M.; Spannenberg, A.; Langer, P.; Iaroshenko, V.O. Novel and efficient synthesis of 4,7-dihydro-1H-pyrrolo[2,3-*b*]pyridine derivatives via one-pot, three-component approach from N-substituted 5-amino-3-cyanopyrroles, various carbonyl and active methylene compounds. *Tetrahedron* **2013**, *69*, 5955–5967, <https://doi.org/10.1016/j.tet.2013.04.115>.
18. Olivieri, P.R.; Hodous, B.L; 1H-Pyrrole-2-carbonitrile. *Encyclopedia of Reagents for Organic Synthesis*, 1999, *44*, 203–208. <https://doi.org/10.1002/047084289X.rn01059>.
19. Xu, X.; Zhang, Y. Convenient preparations of polysubstituted 3H-pyrroles promoted by SmI₂. *J. Chem. Soc., Perkin Trans. I* **2001**, *1*, 2836–2839, <https://doi.org/10.1039/B102268G>.
20. Li, Y.; Zhang, P.; Ma, Q.; Song, H.; Liu, Y.; Wang, Q. The trifluoromethyl transformation synthesis, crystal structure and insecticidal activities of novel 2-pyrrolecarboxamide and 2-pyrrolecarboxlate. *Bioorganic Med. Chem. Lett.* **2012**, *22*, 6858–6861, <https://doi.org/10.1016/j.bmcl.2012.09.036>.
21. Niu, L.; Yi, H.; Wang, S.; Liu, T.; Liu, J.; Lei, A. Photo-induced oxidant-free oxidative C-H/N-H cross-coupling between arenes and azoles. *Nat. Commun.* **2017**, *8*, 14226, <https://doi.org/10.1038/ncomms14226>.
22. Lauria, A.; Bruno, M.; Diana, P.; Barraja, P.; Montalbano, A.; Cirrincione, G.; Dattolo, G.; Almerico, A.M. Annelated pyrrolo-pyrimidines from amino-cyanopyrroles and BMMAAs as leads for new DNA-interactive ring systems. *Bioorganic Med. Chem.* **2005**, *13*, 1545–1553, <https://doi.org/10.1016/j.bmc.2004.12.027>.
23. Yamamoto, T.; Yamashita, R. Preparation of new π-conjugated thiophene-pyrrole copolymers having ethynyl substituents at the N-position of pyrrole. *Polym. J.* **2008**, *40*, 775–778, <https://doi.org/10.1295/polymj.PJ2008003>.
24. Ge, L.; Wang, D.; Xing, R.; Ma, D.; Walsh, P.J. Photoredox-catalyzed oxo-amination of aryl cyclopropanes. *Nat. Commun.* **2019**, *10*, 4367, <https://doi.org/10.1038/s41467-019-12403-2>.
25. Lama, L.; Adura, C.; Xie, W. et al. Development of human cGAS-specific small-molecule inhibitors for repression of dsDNA-triggered interferon expression. *Nat. Commun.* **2019**, *10*, 2261, <https://doi.org/10.1038/s41467-019-08620-4>.
26. Geretto, M.; Ponassi, M.; Casale, M.; Pulliero, A.; Cafeo, G.; Malagreca, F.; Profumo, A.; Balza, E.; Bersimbaev, R.; Kohnke, F.H.; Rosano, C.; Izzotti, A. A novel calix[4]pyrrole derivative as a potential anticancer agent that forms genotoxic adducts with DNA. *Sci. Rep.* **2018**, *8*, 11075, <https://doi.org/10.1038/s41598-018-29314-9>.
27. Hiraoka, K.; Inoue, T.; Taylor, R.D. et al. Inhibition of KRAS codon 12 mutants using a novel DNA-alkylating pyrrole-imidazole polyamide conjugate. *Nat. Commun.* **2015**, *6*, 6706, <https://doi.org/10.1038/ncomms7706>.
28. Pandey, B.; Grover, S.; Goyal, S.; Kumari, A.; Singh, A.; Jamal, S.; Kaur, J.; Grover, A. Alanine mutation of the catalytic sites of Pantothenate Synthetase causes distinct conformational changes in the ATP binding region. *Sci. Rep.* **2018**, *8*, 903, <https://doi.org/10.1038/s41598-017-19075-2>.
29. Shehata, M.A.; Nøhr, A.C.; Lissa, D.; Bisig, C.; Isberg, V.; Andersen, K.B.; Harpsøe, K.; Björkling, F.; Bräuner-Osborne, H.; Gloriam, D.E. Novel agonist bioisosteres and common structure-activity relationships for the orphan G Protein-coupled receptor GPR139. *Sci. Rep.* **2016**, *6*, 36681, <https://doi.org/10.1038/srep36681>.
30. Sasaki, A.; Ide, S.; Kawamoto, Y.; Bando, T.; Murata, Y.; Shimura, M.; Yamada, K.; Hirata, A.; Nokihara, K.; Hirata, T.; Sugiyama, H.; Maeshima, K. Telomere Visualization in Tissue Sections using Pyrrole-

- Imidazole Polyamide Probes. *Sci. Rep.* **2016**, *6*, 29261, <https://doi.org/10.1038/srep29261>.
31. Moya, C.; Santiago, R.; Hospital-Benito, D.; Lemus, J.; Palomar, J. Design of biogas upgrading processes based on ionic liquids. *Chem. Eng. J.* **2022**, *428*, 132103, <https://doi.org/10.1016/j.cej.2021.132103>.
32. Duan, K.; Ning, J.; Zhou, L.; Xu, W.; Feng, C.; Yang, T.; Wang, S.; Liu, J. 1-(2-Cyanoethyl)pyrrole enables excellent battery performance at high temperature: Via the synergistic effect of Lewis base and CN functional groups. *Chem. Commun.* **2020**, *56*, 8420–8423, <https://doi.org/10.1039/D0CC01528H>.
33. Ferin Fathima, A.; Jothi Mani, R.; Sakthipandi, K.; Manimala, K.; Hossain, A. Enhanced Antifungal Activity of Pure and Iron-Doped ZnO Nanoparticles Prepared in the Absence of Reducing Agents. *J. Inorg. Organomet. Polym. Mater.* **2020**, *30*, 2397–2405, <https://doi.org/10.1007/s10904-019-01400-z>.
34. Vinoth Kumar, G.G.; Kesavan, M.P.; Sankarganesh, M.; Sakthipandi, K.; Rajesh, J.; Sivaraman, G. A Schiff base receptor as a fluorescence turn-on sensor for Ni^{2+} ions in living cells and logic gate application. *New J. Chem.* **2018**, *42*, 2865–2873, <https://doi.org/10.1039/C7NJ03784H>.
35. Liu, C.; Chen, Y.; Sun, Y.; Wu, F. Crystal structure and mechanistic investigation of the reaction of 5-amino-1-(2,6-dichloro-4-(trifluoromethyl)phenyl)-1H-pyrazole-3-carbonitrile with unsaturated carbonyl compounds. *Res. Chem. Intermed.* **2013**, *39*, 2087–2093, <http://dx.doi.org/10.1007/s11164-012-0740-5>.
36. Paularokiadoss, F.; Sekar, A.; Christopher Jeyakumar, T. A DFT study on structural and bonding analysis of transition-metal carbonyls with terminal haloborylene ligands $[\text{M}(\text{CO})_3(\text{BX})]$ ($\text{M} = \text{Ni}, \text{Pd}$, and Pt ; $\text{X} = \text{F}, \text{Cl}, \text{Br}$, and I). *Comput. Theor. Chem.* **2020**, *1177*, 112750, <https://doi.org/10.1016/j.comptc.2020.112750>.
37. Saleem, S.H.S.; Sankarganesh, M.; Raja, J.D.; Jose, P.R.A.; Sakthivel, A.; Jeyakumar, T.C.; Asha, R.N. Synthesis, characterization, DFT calculation, biological and molecular docking of $\text{Cu}(\text{II})$ complex of pyrimidine derived Schiff base ligand. *J. Saudi Chem. Soc.* **2021**, *25*, 101225, <https://doi.org/10.1016/j.jscs.2021.101225>.
38. Christopher Jeyakumar, T.; Baskaran, S.; Sivasankar, C. Possibility of reducing the coordinated dinitrogen into ammonia and hydrazine using $[\text{Ru}-\text{L}]$ ($\text{L} = \text{triimidoamine}$) and FLP-H 2 : A DFT study. *J. Chem. Sci.* **2018**, *130*, 57, <https://doi.org/10.1007/s12039-018-1460-1>.
39. Frisch, M.J.; Trucks, G.W.; Schlegel, H.B. et al. Gaussian 09 Revision D.01, **2014**.
40. Frisch, M.J.; Pople, J.A. Self-consistent molecular orbital methods 25. Supplementary functions for Gaussian basis sets. *J. Chem. Phys.* **1984**, *80*, 3265, <https://doi.org/10.1063/1.447079>.
41. Longuet-Higgins, H.C.; Pople, J.A. Electronic Spectral Shifts of Nonpolar Molecules in Nonpolar Solvents. *J. Chem. Phys.* **1957**, *27*, 192, <https://doi.org/10.1063/1.1743666>.
42. Krishnan, R.; Binkley, J.S.; Seeger, R.; Pople, J.A. Self-consistent molecular orbital methods. XX. A basis set for correlated wave functions. *J. Chem. Phys.* **1980**, *72*, 650, <https://doi.org/10.1063/1.438955>.
43. Rassolov, V.A.; Ratner, M.A.; Pople, J.A.; Redfern, P.C.; Curtiss, L.A. 6-31G* basis set for third-row atoms. *J. Comput. Chem.* **2001**, *22*, 976–984, <https://doi.org/10.1002/jcc.1058>.
44. Ditchfield, R.; Hehre, W.J.; Pople, J.A. Self-Consistent Molecular-Orbital Methods. IX. An Extended Gaussian-Type Basis for Molecular-Orbital Studies of Organic Molecules. *J. Chem. Phys.* **1971**, *54*, 724, <https://doi.org/10.1063/1.1674902>.
45. Becke, A.D. Density-functional thermochemistry. III. The role of exact exchange. *J. Chem. Phys.* **1993**, *98*, 5648, <https://doi.org/10.1063/1.464913>.
46. Schmid, H.L.; Becke, A.D. Chemical content of the kinetic energy density. *J. Mol. Struct.: THEOCHEM* **2000**, *527*, 51–61, [https://doi.org/10.1016/S0166-1280\(00\)00477-2](https://doi.org/10.1016/S0166-1280(00)00477-2).
47. Becke, A.D. Density-functional exchange-energy approximation with correct asymptotic behavior. *Phys. Rev. A* **1988**, *38*, 3098–3100, <https://doi.org/10.1103/PhysRevA.38.3098>.
48. Becke, A.D.; Johnson, E.R. A density-functional model of the dispersion interaction. *J. Chem. Phys.* **2005**, *123*, 154101, <https://doi.org/10.1063/1.2065267>.
49. Becke, A.D. Perspective: Fifty years of density-functional theory in chemical physics. *J. Chem. Phys.* **2014**, *140*, 18A301, <https://doi.org/10.1063/1.4869598>.
50. Yanai, T.; Tew, D.P.; Handy, N.C. A new hybrid exchange–correlation functional using the Coulomb-attenuating method (CAM-B3LYP). *Chem. Phys. Lett.* **2004**, *393*, 51–57, <https://doi.org/10.1016/j.cplett.2004.06.011>.
51. Okuno, K.; Shigeta, Y.; Kishi, R.; Miyasaka, H.; Nakano, M. Tuned CAM-B3LYP functional in the time-dependent density functional theory scheme for excitation energies and properties of diarylethene derivatives. *J. Photochem. Photobiol. A: Chem.* **2012**, *235*, 29–34, <https://doi.org/10.1016/j.jphotochem.2012.03.003>.
52. O'boyle, N.M.; Tenderholt, A.L.; Langner, K.M. cclib: A library for package-independent computational chemistry algorithms. *J. Comput. Chem.* **2008**, *29*, 839–845, <https://doi.org/10.1002/jcc.20823>.

53. Lu, T.; Chen, F. Multiwfn: A multifunctional wavefunction analyzer. *J. Comput. Chem.* **2012**, *33*, 580–592, <https://doi.org/10.1002/jcc.22885>.
54. Burley, S.K.; Berman, H.M.; Bhikadiya, C. et al. RCSB Protein Data Bank: biological macromolecular structures enabling research and education in fundamental biology, biomedicine, biotechnology and energy. *Nucleic Acids Res.* **2018**, *47*, D464–D474, <https://doi.org/10.1093/nar/gky1004>.
55. Trott, O.; Olson, A.J. AutoDock Vina: Improving the speed and accuracy of docking with a new scoring function, efficient optimization, and multithreading. *J. Comput. Chem.* **2010**, *31*, 455–461, <https://doi.org/10.1002/jcc.21334>.
56. Discovery Studio BIOVIA. *Discov. Stud. Client v17, San Diego, Dassault Syst.* **2017**.
57. Kumar, V.S.; Mary, Y.S.; Pradhan, K.; Brahman, D.; Mary, Y.S.; Thomas, R.; Roxy, M.S.; Van Alsenoy, C. Van Synthesis, spectral properties, chemical descriptors and light harvesting studies of a new bioactive azo imidazole compound. *J. Mol. Struct.* **2020**, *1199*, 127035, <https://doi.org/10.1016/j.molstruc.2019.127035>.
58. Afzal, A.; Thayyil, M.S.; Shariq, M.; Mary, Y.S.; Resmi, K.S.; Thomas, R.; Islam, N.; Abinu, A.J. Anti-Cancerous Brucine and Colchicine: Experimental and Theoretical Characterization. *ChemistrySelect* **2019**, *4*, 11441–11454, <https://doi.org/10.1002/slct.201902698>.
59. Mary, Y.S.; Yalcin, G.; Mary, Y.S.; Resmi, K.S.; Thomas, R.; Önkol, T.; Kasap, E.N.; Yildiz, I. Spectroscopic, quantum mechanical studies, ligand protein interactions and photovoltaic efficiency modeling of some bioactive benzothiazolinone acetamide analogs. *Chem. Pap.* **2020**, *74*, 1957–1964, <https://doi.org/10.1007/s11696-019-01047-7>.
60. Priya, Y.S.; Rao, K.R.; Chalapathi, P. V; Veeraiah, A.; Srikanth, K.E.; Mary, Y.S.; Thomas, R. Intricate spectroscopic profiling, light harvesting studies and other quantum mechanical properties of 3-phenyl-5-isooxazolone using experimental and computational strategies. *J. Mol. Struct.* **2020**, *1203*, 127461, <https://doi.org/10.1016/j.molstruc.2019.127461>.
61. Thomas, R.; Mary, Y.S.; Resmi, K.S.; Narayana, B.; Sarojini, B.K.; Vijayakumar, G.; Van Alsenoy, C. Two neoteric pyrazole compounds as potential anticancer agents: Synthesis, electronic structure, physico-chemical properties and docking analysis. *J. Mol. Struct.* **2019**, *1181*, 455–466, <https://doi.org/10.1016/j.molstruc.2019.01.003>.
62. Al-Otaibi, J.S.; Mary, Y.S.; Armaković, S.; Thomas, R. Hybrid and bioactive cocrystals of pyrazinamide with hydroxybenzoic acids: Detailed study of structure, spectroscopic characteristics, other potential applications and non-covalent interactions using SAPT. *J. Mol. Struct.* **2020**, *1202*, 127316, <https://doi.org/10.1016/j.molstruc.2019.127316>.
63. Sun, C.; Li, Y.; Song, P.; Ma, F. An experimental and theoretical investigation of the electronic structures and photoelectrical properties of ethyl red and carminic acid for DSSC application. *Materials* **2016**, *9*, 813, <https://doi.org/10.3390/ma9100813>.
64. dos Santos, G.C.; Oliveira, E.F.; Lavarda, F.C.; da Silva-Filho, L.C. Designing new quinoline-based organic photosensitizers for dye-sensitized solar cells (DSSC): a theoretical investigation. *J. Mol. Model.* **2019**, *25*, 75, <https://doi.org/10.1007/s00894-019-3958-y>.
65. Curutchet, C.; Mennucci, B. Quantum chemical studies of light harvesting. *Chem. Rev.* **2017**, *117*, 294–343, <https://doi.org/10.1021/acs.chemrev.5b00700>.
66. Chako, N.Q. Absorption of Light in Organic Compounds. *J. Chem. Phys.* **1934**, *2*, 644–653, <https://doi.org/10.1063/1.1749368>.
67. Rho, Y.; Wanit, M.; Yeo, J.; Hong, S.; Han, S.; Choi, J.-H.; Hong, W.-H.; Lee, D.; Ko, S.H. Improvement of light-harvesting efficiency in dye-sensitized solar cells using silica beads embedded in a TiO₂ nanoporous structure. *J. Phys. D: Appl. Phys.* **2013**, *46*, 024006, <http://dx.doi.org/10.1088/0022-3727/46/2/024006>.
68. Al-Zaqri, N.; Pooventhiran, T.; Alharthi, F.A.; Bhattacharyya, U.; Thomas, R. Structural investigations, quantum mechanical studies on proton and metal affinity and biological activity predictions of selpercatinib. *J. Mol. Liq.* **2021**, *325*, 114765, <https://doi.org/10.1016/j.molliq.2020.114765>.
69. Al-Zaqri, N.; Pooventhiran, T.; Rao, D.J.; Alsalme, A.; Warad, I.; Thomas, R. Structure, conformational dynamics, quantum mechanical studies and potential biological activity analysis of multiple sclerosis medicine ozanimod. *J. Mol. Struct.* **2021**, *1227*, 129685, <https://doi.org/10.1016/j.molstruc.2020.129685>.
70. Bhattacharyya, U.; Pooventhiran, T.; Thomas, R. Adsorption of the drug bempedoic acid over different 2D/3D nanosurfaces and enhancement of Raman activity enabling ultrasensitive detection: First principle analysis. *Spectrochim. Acta - Part A: Mol. Biomol. Spectrosc.* **2021**, *254*, 119630, <https://doi.org/10.1016/j.saa.2021.119630>.
71. Pooventhiran, T.; Al-Zaqri, N.; Alsalme, A.; Bhattacharyya, U.; Thomas, R. Structural aspects,

- conformational preference and other physico-chemical properties of Artesunate and the formation of self-assembly with graphene quantum dots : A first principle analysis and surface enhancement of Raman activity investigation. *J. Mol. Liq.* **2021**, 325, 114810, <https://doi.org/10.1016/j.molliq.2020.114810>.
72. Alsalme, A.; Pooventhiran, T.; Al-Zaqri, N.; Rao, D.J.; Thomas, R. Structural, physico-chemical landscapes , ground state and excited state properties in different solvent atmosphere of Avapritinib and its ultrasensitive detection using SERS / GERS on self-assembly formation with graphene quantum dots. *J. Mol. Liq.* **2021**, 322, 114555, <https://doi.org/10.1016/j.molliq.2020.114555>.
73. Pooventhiran, T.; Cheriet, M.; Bhattacharyya, U.; Irfan, A.; Puchta, R.; Sowrirajan, S.; Thomas, R. Detailed Structural Examination, Quantum Mechanical Studies of the Aromatic Compound Solarimfetol and Formation of Inclusion Compound with Cucurbituril. *Polycycl. Aromat. Compd.* **2022**, (In press) <https://doi.org/10.1080/10406638.2021.1937238>.
74. Alharthi, F.A.; Al-Zaqri, N.; Alsalme, A.; Al-Taleb, A.; Pooventhiran, T.; Thomas, R.; Rao, D.J. Excited-state electronic properties , structural studies , non-covalent interactions , and inhibition of the novel severe acute respiratory syndrome coronavirus 2 proteins in Ripretinib by first-principle simulations. *J. Mol. Liq.* **2021**, 324, 115134, <https://doi.org/10.1016/j.molliq.2020.115134>.
75. Al-Zaqri, N.; Pooventhiran, T.; Alsalme, A.; Warad, I.; John, A.M.; Thomas, R. Structural and physico-chemical evaluation of melatonin and its solution-state excited properties , with emphasis on its binding with novel coronavirus proteins. *J. Mol. Liq.* **2020**, 318, 114082, <https://doi.org/10.1016/j.molliq.2020.114082>.
76. Pooventhiran, T.; Bhattacharyya, U.; Rao, D.J.; Chandramohan, V.; Karunakar, P.; Irfan, A.; Mary, Y.S.; Thomas, R. Detailed spectra, electronic properties, qualitative non-covalent interaction analysis, solvatochromism, docking and molecular dynamics simulations in different solvent atmosphere of cenobamate. *Struct. Chem.* **2020**, 31, 2475–2485, <https://doi.org/10.1007/s11224-020-01607-8>.
77. Surendar, P.; Pooventhiran, T.; Rajam, S.; Bhattacharyya, U.; Bakht, A.; Thomas, R. Quasi liquid Schiff bases from trans -2-hexenal and cytosine and 1 -leucine with potential antieczematic and antiarthritic activities: Synthesis , structure and quantum mechanical studies. *J. Mol. Liq.* **2021**, 334, 116448, <https://doi.org/10.1016/j.molliq.2021.116448>.
78. Surendar, P.; Pooventhiran, T.; Al-Zaqri, N.; Rajam, S.; Jagadeeswara Rao, D.; Thomas, R. Synthesis of three quasi liquid Schiff bases between hexanal and adenine, cytosine, and 1-leucine, structural interpretation, quantum mechanical studies and biological activity prediction. *J. Mol. Liq.* **2021**, 341, 117305, <https://doi.org/10.1016/j.molliq.2021.117305>.
79. Thomas, R.; Pooventhiran, T.; El-bahy, S.M.; El Azab, I.H.; Mersal, G.A.M.; Ibrahim, M.M.; El-Bahy, Z.M. Evidence of significant non-covalent interactions in the solution of Levetiracetam in water and methanol. *J. Mol. Liq.* **2022**, 359, 119289, <https://doi.org/10.1016/j.molliq.2022.119289>.
80. Pooventhiran, T.; Thomas, R. Hydrogen bonds between valsartan and solvents (water and methanol): Evidences for solvation dynamics using local energy decomposition and ab initio molecular dynamics analysis. *J. Mol. Liq.* **2022**, 354, 118856, <https://doi.org/10.1016/j.molliq.2022.118856>.
81. Pooventhiran, T.; Gangadharappa, B.S.; Abu Ali, O.A.; Thomas, R.; Saleh, D.I. Study of the structural features and solvent effects using ab initio molecular dynamics and energy decomposition analysis of Atogepant in water and ammonia. *J. Mol. Liq.* **2022**, 352, 118672, <https://doi.org/10.1016/j.molliq.2022.118672>.
82. Alsalme, A.; Pooventhiran, T.; Al-Zaqri, N.; Rao, D.J.; Rao, S.S.; Thomas, R. Modelling the structural and reactivity landscapes of tucatinib with special reference to its wavefunction-dependent properties and screening for potential antiviral activity. *J. Mol. Model.* **2020**, 26, 341, <https://doi.org/10.1007/s00894-020-04603-1>.
83. Al-Zaqri, N.; Pooventhiran, T.; Alsalme, A.; Rao, D.J.; Rao, S.S.; Sankar, A.; Thomas, R. First-Principle Studies of Istradefylline with Emphasis on the Stability, Reactivity, Interactions and Wavefunction-Dependent Properties. *Polycycl. Aromat. Compd.* **2022**, (In press) <https://doi.org/10.1080/10406638.2020.1857273>.
84. Li, H.; Van Vranken, S.; Zhao, Y.; Li, Z.; Guo, Y.; Eisele, L.; Li, Y. Crystal structures of T cell receptor β chains related to rheumatoid arthritis. *Protein Sci.* **2005**, 14, 3025–3038, <https://doi.org/10.1110/ps.051748305>.
85. Yeddu, S.P.; Pooventhiran, T.; Veeraiah, A.; Vijay, D.; Srikanth, K.E.; Irfan, A.; Thomas, R. Vibrational Spectral Studies, Quantum Mechanical Properties, and Biological Activity Prediction and Inclusion Molecular Self-Assembly Formation of N-N'-Dimethylethylene Urea. *Biointerface Res. Appl. Chem.* **2022**, 12, 3996–4017, <https://doi.org/10.33263/BRIAC123.39964017>.

86. Pooventhiran, T.; Marondedze, E.F.; Govender, P.P.; Bhattacharyya, U.; Rao, D.J.; Aazam, E.S.; Kuthanapillil, J.M.; E, T.J.; Thomas, R. Energy and reactivity profile and proton affinity analysis of rimegepant with special reference to its potential activity against SARS-CoV-2 virus proteins using molecular dynamics. *J. Mol. Model.* **2021**, *27*, 276, <https://doi.org/10.1007/s00894-021-04885-z>.
87. Loke, S.K.; Pagadala, E.; Srinivasadesikan, V.; Thanapaul, R.J.R.S.; Pooventhiran, T.; Thomas, R.; Naganjaneyulu, G.; Kottalanka, R.K. Unprecedented biological evaluation of Zn (II) complexes supported by "Self-adjustable" acyclic diiminodipyrromethane Schiff's bases: DFT, molecular docking ; biological activity studies. *Inorg. Chem. Commun.* **2021**, *133*, 108936, <https://doi.org/10.1016/j.inoche.2021.108936>.
88. Bakht, M.A.; Azam, F.; Ali, A.; Thomas, R.; Pooventhiran, T.; Ali, A.; Ahsan, M.A. Synthesis and biological studies of oxoquinolines: Experimental and theoretical investigations. *J. Mol. Struct.* **2022**, *1248*, 131509, <https://doi.org/10.1016/j.molstruc.2021.131509>.
89. Suryanarayana, K.; Robert, A.R.; Kerru, N.; Pooventhiran, T.; Thomas, R.; Maddila, S.; Jonnalagadda, S.B. Design, synthesis, anticancer activity and molecular docking analysis of novel dinitrophenylpyrazole bearing 1,2,3-triazoles. *J. Mol. Struct.* **2021**, *1243*, 130865, <https://doi.org/10.1016/j.molstruc.2021.130865>.

Supplementary materials

Table S1. Natural atomic orbital occupancies of carbonitrile

NAOs	Atom	No.	lang	Type(AO)	Occupancy	Energy	NAOs	Atom	No.	lang	Type(AO)	Occupancy	Energy
1	C	1	S	C(1S)	1.99888	-10.0836	283	Cl	13	S	C(1S)	2	-100.3
2	C	1	S	V(2S)	0.93626	-0.21181	284	Cl	13	S	C(2S)	1.99969	-10.4811
3	C	1	S	R(4S)	0.00196	1.13995	285	Cl	13	S	V(3S)	1.83455	-1.03965
4	C	1	S	R(3S)	0.00015	1.08019	286	Cl	13	S	R(5S)	0.00135	1.28151
5	C	1	S	R(5S)	0.00002	21.40866	287	Cl	13	S	R(4S)	0.0001	0.74922
6	C	1	px	V(2p)	1.09893	-0.12909	288	Cl	13	S	R(6S)	0	17.54267
7	C	1	px	R(4p)	0.00489	0.92613	289	Cl	13	S	R(7S)	0	207.7893
8	C	1	px	R(3p)	0.00034	0.6228	290	Cl	13	px	C(2p)	1.99998	-7.2611
9	C	1	px	R(5p)	0.00015	3.40573	291	Cl	13	px	V(3p)	1.80778	-0.34672
10	C	1	py	V(2p)	1.15807	-0.1234	292	Cl	13	px	R(4p)	0.00236	0.53853
11	C	1	py	R(4p)	0.00656	1.02544	293	Cl	13	px	R(5p)	0.00012	0.73345
12	C	1	py	R(3p)	0.00034	0.52004	294	Cl	13	px	R(6p)	0.00002	2.84702
13	C	1	py	R(5p)	0.0001	3.41363	295	Cl	13	px	R(7p)	0	25.46366
14	C	1	pz	V(2p)	0.98859	-0.16529	296	Cl	13	py	C(2p)	1.99993	-7.26616
15	C	1	pz	R(4p)	0.00118	0.49715	297	Cl	13	py	V(3p)	1.37149	-0.3183
16	C	1	pz	R(3p)	0.00047	0.33973	298	Cl	13	py	R(4p)	0.00266	0.46155
17	C	1	pz	R(5p)	0.00003	2.80662	299	Cl	13	py	R(5p)	0.00009	0.53911
18	C	1	dxy	R(3d)	0.001	2.05483	300	Cl	13	py	R(6p)	0.00005	3.43001
19	C	1	dxy	R(4d)	0.00054	3.63768	301	Cl	13	py	R(7p)	0	25.48849
20	C	1	dxz	R(3d)	0.00038	1.32281	302	Cl	13	pz	C(2p)	1.99999	-7.26012
21	C	1	dxz	R(4d)	0.00016	3.0867	303	Cl	13	pz	V(3p)	1.91241	-0.35849
22	C	1	dyz	R(3d)	0.00055	1.27964	304	Cl	13	pz	R(4p)	0.00205	0.47158
23	C	1	dyz	R(4d)	0.00009	3.04273	305	Cl	13	pz	R(5p)	0.00012	0.57922
24	C	1	dx2y2	R(3d)	0.00103	2.01078	306	Cl	13	pz	R(6p)	0.00004	2.40184
25	C	1	dx2y2	R(4d)	0.00044	3.60032	307	Cl	13	pz	R(7p)	0	25.3405

26	C	1	dz2	R(3d)	0.00158	1.69733		308	Cl	13	dxy	R(3d)	0.00245	1.44879
27	C	1	dz2	R(4d)	0.00006	3.31712		309	Cl	13	dxy	R(4d)	0.00005	2.66364
								310	Cl	13	dxz	R(3d)	0.00087	0.77428
28	C	2	S	C(1S)	1.99886	-10.1089		311	Cl	13	dxz	R(4d)	0.00005	2.22838
29	C	2	S	V(2S)	0.90131	-0.21571		312	Cl	13	dyz	R(3d)	0.00238	0.89038
30	C	2	S	R(4S)	0.00091	1.27092		313	Cl	13	dyz	R(4d)	0.00004	2.38694
31	C	2	S	R(3S)	0.00013	0.94282		314	Cl	13	dx2y2	R(3d)	0.00176	1.31952
32	C	2	S	R(5S)	0.00001	21.29905		315	Cl	13	dx2y2	R(4d)	0.00003	2.65318
33	C	2	px	V(2p)	1.04758	-0.15027		316	Cl	13	dz2	R(3d)	0.00109	1.01894
34	C	2	px	R(4p)	0.0061	1.16703		317	Cl	13	dz2	R(4d)	0.00006	2.39895
35	C	2	px	R(3p)	0.00028	0.68988		318	Cl	14	S	C(1S)	2	-100.292
36	C	2	px	R(5p)	0.00017	3.47503		319	Cl	14	S	C(2S)	1.99968	-10.4753
37	C	2	py	V(2p)	1.09881	-0.12557		320	Cl	14	S	V(3S)	1.83234	-1.02971
38	C	2	py	R(4p)	0.00411	1.15754		321	Cl	14	S	R(5S)	0.0014	1.28111
39	C	2	py	R(3p)	0.00054	0.59008		322	Cl	14	S	R(4S)	0.00005	0.77545
40	C	2	py	R(5p)	0.0002	3.58332		323	Cl	14	S	R(6S)	0	17.61978
41	C	2	pz	V(2p)	1.03255	-0.17336		324	Cl	14	S	R(7S)	0	207.7259
42	C	2	pz	R(4p)	0.00198	0.57599		325	Cl	14	px	C(2p)	1.99997	-7.25412
43	C	2	pz	R(3p)	0.0004	0.4872		326	Cl	14	px	V(3p)	1.77654	-0.33645
44	C	2	pz	R(5p)	0.00001	2.75777		327	Cl	14	px	R(4p)	0.00246	0.54988
45	C	2	dxy	R(3d)	0.001	1.92471		328	Cl	14	px	R(5p)	0.00013	0.89279
46	C	2	dxy	R(4d)	0.00064	3.65781		329	Cl	14	px	R(6p)	0.00002	2.73389
47	C	2	dxz	R(3d)	0.001	1.02273		330	Cl	14	px	R(7p)	0	25.47041
48	C	2	dxz	R(4d)	0.00018	3.42411		331	Cl	14	py	C(2p)	1.99993	-7.25846
49	C	2	dyz	R(3d)	0.00052	1.06608		332	Cl	14	py	V(3p)	1.4092	-0.31313
50	C	2	dyz	R(4d)	0.0003	3.36388		333	Cl	14	py	R(4p)	0.00254	0.47963
51	C	2	dx2y2	R(3d)	0.00154	2.00471		334	Cl	14	py	R(5p)	0.0001	0.70455
52	C	2	dx2y2	R(4d)	0.00076	3.60066		335	Cl	14	py	R(6p)	0.00004	3.23476
53	C	2	dz2	R(3d)	0.00215	1.52176								

82	C	4	S	C(1S)	1.99847	-10.1588	364	C	15	py	R(3p)	0.00048	0.56574
83	C	4	S	V(2S)	0.92197	-0.26167	365	C	15	py	R(5p)	0.00012	2.69023
84	C	4	S	R(4S)	0.00107	1.13222	366	C	15	pz	V(2p)	0.83449	-0.06514
85	C	4	S	R(3S)	0.0001	0.87072	367	C	15	pz	R(4p)	0.00532	1.08222
86	C	4	S	R(5S)	0.00002	21.9502	368	C	15	pz	R(3p)	0.00023	0.73195
87	C	4	px	V(2p)	1.05037	-0.15176	369	C	15	pz	R(5p)	0.00014	3.00149
88	C	4	px	R(4p)	0.00566	0.91499	370	C	15	dxy	R(4d)	0.00096	2.30809
89	C	4	px	R(3p)	0.00012	0.64037	371	C	15	dxy	R(3d)	0.00009	2.30603
90	C	4	px	R(5p)	0.00017	3.64336	372	C	15	dxz	R(3d)	0.00103	2.53033
91	C	4	py	V(2p)	0.98012	-0.18272	373	C	15	dxz	R(4d)	0.00053	3.20626
92	C	4	py	R(4p)	0.0071	0.92682	374	C	15	dyz	R(3d)	0.00099	2.38837
93	C	4	py	R(3p)	0.00023	0.50019	375	C	15	dyz	R(4d)	0.00029	2.45107
94	C	4	py	R(5p)	0.0002	3.53601	376	C	15	dx2y2	R(3d)	0.00068	2.66521
95	C	4	pz	V(2p)	1.02784	-0.19171	377	C	15	dx2y2	R(4d)	0.0004	2.84163
96	C	4	pz	R(4p)	0.00142	0.55518	378	C	15	dz2	R(3d)	0.00074	2.5782
97	C	4	pz	R(3p)	0.00032	0.40241	379	C	15	dz2	R(4d)	0.00054	3.14866
98	C	4	pz	R(5p)	0.00003	2.80089							
99	C	4	dxy	R(3d)	0.00247	1.81746	380	C	16	S	C(1S)	1.99897	-10.11114
100	C	4	dxy	R(4d)	0.00056	3.70609	381	C	16	S	V(2S)	0.85096	-0.15231
101	C	4	dxz	R(3d)	0.00109	1.07916	382	C	16	S	R(3S)	0.00232	1.10068
102	C	4	dxz	R(4d)	0.0002	3.32665	383	C	16	S	R(4S)	0.00005	1.77108
103	C	4	dyz	R(3d)	0.00213	1.04104	384	C	16	S	R(5S)	0.00003	20.73281
104	C	4	dyz	R(4d)	0.00014	3.34003	385	C	16	px	V(2p)	0.96479	-0.07965
105	C	4	dx2y2	R(3d)	0.00221	1.82005	386	C	16	px	R(4p)	0.00604	1.42057
106	C	4	dx2y2	R(4d)	0.00045	3.7345	387	C	16	px	R(3p)	0.00009	0.62878
107	C	4	dz2	R(3d)	0.00331	1.51633	388	C	16	px	R(5p)	0.00016	2.91855
108	C	4	dz2	R(4d)	0.00012	3.4819	389	C	16	py	V(2p)	1.06086	-0.14268
							390	C	16	py	R(4p)	0.00136	0.74204
							391	C	16	py	R(3p)	0.00039	0.55144

109	C	5	S	C(1S)	1.9986	-10.132	392	C	16	py	R(5p)	0.00008	2.69531
110	C	5	S	V(2S)	0.81841	-0.17657	393	C	16	 pz	V(2p)	1.06428	-0.09654
111	C	5	S	R(3S)	0.00155	1.13284	394	C	16	pz	R(4p)	0.00584	1.48357
112	C	5	S	R(4S)	0.00004	5.28665	395	C	16	pz	R(3p)	0.00014	0.77397
113	C	5	S	R(5S)	0.00002	16.98713	396	C	16	pz	R(5p)	0.00015	2.72971
114	C	5	px	V(2p)	0.88882	-0.09883	397	C	16	dxy	R(3d)	0.00074	1.82372
115	C	5	px	R(3p)	0.00691	1.15584	398	C	16	dxy	R(4d)	0.00009	2.76
116	C	5	px	R(5p)	0.00009	2.90052	399	C	16	dxz	R(3d)	0.00116	2.39067
117	C	5	px	R(4p)	0.00011	1.66119	400	C	16	dxz	R(4d)	0.00058	3.71898
118	C	5	py	V(2p)	1.10987	-0.15347	401	C	16	dyz	R(3d)	0.00091	1.86185
119	C	5	py	R(3p)	0.00522	1.06829	402	C	16	dyz	R(4d)	0.00011	2.79937
120	C	5	py	R(5p)	0.00025	2.61401	403	C	16	dx2y2	R(3d)	0.00112	2.13672
121	C	5	py	R(4p)	0.0001	1.62316	404	C	16	dx2y2	R(4d)	0.00033	3.24273
122	C	5	 pz	V(2p)	1.05644	-0.17797	405	C	16	dz2	R(3d)	0.00063	2.22463
123	C	5	pz	R(3p)	0.00595	0.61521	406	C	16	dz2	R(4d)	0.00038	3.19333
124	C	5	pz	R(5p)	0.00007	2.21431							
125	C	5	pz	R(4p)	0.0001	1.44274	407	C	17	S	C(1S)	1.99894	-10.0501
126	C	5	dxy	R(3d)	0.00113	2.29751	408	C	17	S	V(2S)	0.94832	-0.1884
127	C	5	dxy	R(4d)	0.0004	3.58553	409	C	17	S	R(4S)	0.00091	1.36621
128	C	5	dxz	R(3d)	0.00053	1.87047	410	C	17	S	R(3S)	0.00007	1.17105
129	C	5	dxz	R(4d)	0.00051	2.94642	411	C	17	S	R(5S)	0.00001	21.77852
130	C	5	dyz	R(3d)	0.00043	1.74025	412	C	17	px	V(2p)	1.13319	-0.09621
131	C	5	dyz	R(4d)	0.00017	2.71757	413	C	17	px	R(4p)	0.00319	1.18987
132	C	5	dx2y2	R(3d)	0.00155	2.18745	414	C	17	px	R(3p)	0.00044	0.93633
133	C	5	dx2y2	R(4d)	0.00082	3.47509	415	C	17	px	R(5p)	0.0001	2.97614
134	C	5	dz2	R(3d)	0.00093	2.16249	416	C	17	py	V(2p)	1.14558	-0.13931
135	C	5	dz2	R(4d)	0.00033	3.14192	417	C	17	py	R(3p)	0.00228	0.53537
							418	C	17	py	R(4p)	0.00054	0.64378
136	C	6	S	C(1S)	1.99846	-10.1606	419	C	17	py	R(5p)	0.00002	2.52287

137	C	6	S	V(2S)	0.9226	-0.26519	420	C	17	 pz	V(2p)	1.08009	-0.09299
138	C	6	S	R(4S)	0.00108	1.13036	421	C	17	pz	R(4p)	0.00376	0.96451
139	C	6	S	R(3S)	0.0001	0.9248	422	C	17	pz	R(3p)	0.00031	0.95692
140	C	6	S	R(5S)	0.00002	21.94662	423	C	17	pz	R(5p)	0.0001	2.94419
141	C	6	px	V(2p)	1.05592	-0.15188	424	C	17	dxy	R(3d)	0.0008	1.2686
142	C	6	px	R(4p)	0.00558	0.90354	425	C	17	dxy	R(4d)	0.00008	3.17596
143	C	6	px	R(3p)	0.00014	0.65234	426	C	17	dxz	R(3d)	0.00077	1.86213
144	C	6	px	R(5p)	0.00016	3.64275	427	C	17	dxz	R(4d)	0.00052	3.71095
145	C	6	py	V(2p)	0.96816	-0.19038	428	C	17	dyz	R(3d)	0.00067	1.36081
146	C	6	py	R(4p)	0.00695	0.92568	429	C	17	dyz	R(4d)	0.00007	3.19731
147	C	6	py	R(3p)	0.00031	0.51047	430	C	17	dx2y2	R(3d)	0.00189	1.8976
148	C	6	py	R(5p)	0.0002	3.51405	431	C	17	dx2y2	R(4d)	0.00014	3.48732
149	C	6	pz	V(2p)	1.04582	-0.19556	432	C	17	dz2	R(3d)	0.00107	1.84634
150	C	6	pz	R(4p)	0.00141	0.5431	433	C	17	dz2	R(4d)	0.00019	3.49065
151	C	6	pz	R(3p)	0.00033	0.41203							
152	C	6	pz	R(5p)	0.00003	2.79888	434	H	18	S	V(1S)	0.76496	0.02399
153	C	6	dxy	R(3d)	0.00245	1.79684	435	H	18	S	R(3S)	0.00037	1.55622
154	C	6	dxy	R(4d)	0.00054	3.70632	436	H	18	S	R(2S)	0.00017	1.25753
155	C	6	dxz	R(3d)	0.00097	1.10888	437	H	18	px	R(2p)	0.00029	2.78106
156	C	6	dxz	R(4d)	0.00022	3.33363	438	H	18	py	R(2p)	0.00033	2.03321
157	C	6	dyz	R(3d)	0.00211	1.04096	439	H	18	pz	R(2p)	0.00019	2.5961
158	C	6	dyz	R(4d)	0.00015	3.33367							
159	C	6	dx2y2	R(3d)	0.0023	1.81252	440	N	19	S	C(1S)	1.99941	-14.1776
160	C	6	dx2y2	R(4d)	0.00045	3.7313	441	N	19	S	V(2S)	1.43427	-0.55607
161	C	6	dz2	R(3d)	0.00329	1.49806	442	N	19	S	R(4S)	0.0014	2.1719
162	C	6	dz2	R(4d)	0.00011	3.48867	443	N	19	S	R(3S)	0.00004	1.07853
							444	N	19	S	R(5S)	0	35.22353
163	H	7	S	V(1S)	0.75123	0.00949	445	N	19	px	V(2p)	1.14731	-0.18023
164	H	7	S	R(2S)	0.00101	1.21593	446	N	19	px	R(4p)	0.00368	1.02689

165	H	7	S	R(3S)	0.0002	1.69627		447	N	19	px	R(3p)	0.00207	0.56795
166	H	7	px	R(2p)	0.00017	2.65398		448	N	19	px	R(5p)	0.00004	4.70778
167	H	7	py	R(2p)	0.00029	2.80824		449	N	19	py	V(2p)	1.26246	-0.211
168	H	7	pz	R(2p)	0.00026	1.92662		450	N	19	py	R(4p)	0.00183	0.64572
								451	N	19	py	R(3p)	0.00044	0.47089
169	H	8	S	V(1S)	0.75071	0.01185		452	N	19	py	R(5p)	0.00001	3.91124
170	H	8	S	R(2S)	0.00105	1.21945		453	N	19	pz	V(2p)	1.37985	-0.20507
171	H	8	S	R(3S)	0.0002	1.70677		454	N	19	pz	R(4p)	0.00376	0.72946
172	H	8	px	R(2p)	0.00016	2.64087		455	N	19	pz	R(3p)	0.00093	0.52776
173	H	8	py	R(2p)	0.00031	2.83702		456	N	19	pz	R(5p)	0.00003	4.4219
174	H	8	pz	R(2p)	0.00025	1.91803		457	N	19	dxy	R(3d)	0.00123	1.41507
								458	N	19	dxy	R(4d)	0.00011	4.90897
175	C	9	S	C(1S)	1.99913	-10.3691		459	N	19	dxz	R(3d)	0.00441	1.93671
176	C	9	S	V(2S)	0.77691	-0.28519		460	N	19	dxz	R(4d)	0.00022	5.21475
177	C	9	S	R(4S)	0.00389	1.10922		461	N	19	dyz	R(3d)	0.00384	1.44601
178	C	9	S	R(3S)	0.00035	0.86607		462	N	19	dyz	R(4d)	0.00006	4.90723
179	C	9	S	R(5S)	0.00003	22.39807		463	N	19	dx2y2	R(3d)	0.00274	1.68873
180	C	9	px	V(2p)	0.89309	-0.1743		464	N	19	dx2y2	R(4d)	0.00006	5.00591
181	C	9	px	R(4p)	0.00855	1.30815		465	N	19	dz2	R(3d)	0.00498	1.7052
182	C	9	px	R(3p)	0.00054	0.356		466	N	19	dz2	R(4d)	0.00016	5.11639
183	C	9	px	R(5p)	0.00014	1.72078								
184	C	9	py	V(2p)	0.59078	-0.15673		467	N	20	S	C(1S)	1.99914	-14.2565
185	C	9	py	R(4p)	0.01264	1.27091		468	N	20	S	V(2S)	1.14931	-0.53515
186	C	9	py	R(3p)	0.00066	0.40578		469	N	20	S	R(3S)	0.00569	0.72782
187	C	9	py	R(5p)	0.00013	2.32739		470	N	20	S	R(4S)	0.0003	1.86397
188	C	9	pz	V(2p)	0.60271	-0.15454		471	N	20	S	R(5S)	0	34.99592
189	C	9	pz	R(4p)	0.01039	1.1636		472	N	20	px	V(2p)	1.26057	-0.29598
190	C	9	pz	R(3p)	0.00079	0.37601		473	N	20	px	R(4p)	0.00434	1.37462
191	C	9	pz	R(5p)	0.00005	2.24878		474	N	20	px	R(3p)	0.00121	0.80999

192	C	9	dxy	R(3d)	0.00199	2.84112		475	N	20	px	R(5p)	0.00008	4.12125
193	C	9	dxy	R(4d)	0.00024	3.02793		476	N	20	py	V(2p)	1.57563	-0.30388
194	C	9	dxz	R(3d)	0.00271	2.58081		477	N	20	py	R(4p)	0.00608	0.75122
195	C	9	dxz	R(4d)	0.00022	2.80475		478	N	20	py	R(3p)	0.00172	0.52772
196	C	9	dyz	R(3d)	0.00365	2.65548		479	N	20	py	R(5p)	0.00002	3.99139
197	C	9	dyz	R(4d)	0.00035	2.71562		480	N	20	pz	V(2p)	1.23909	-0.29058
198	C	9	dx2y2	R(3d)	0.00262	2.87754		481	N	20	pz	R(4p)	0.00453	0.99805
199	C	9	dx2y2	R(4d)	0.00021	2.92368		482	N	20	pz	R(3p)	0.00115	0.52666
200	C	9	dz2	R(3d)	0.00332	2.62498		483	N	20	pz	R(5p)	0.00004	4.20867
201	C	9	dz2	R(4d)	0.00029	2.90183		484	N	20	dxy	R(3d)	0.00079	1.67418
								485	N	20	dxy	R(4d)	0.00016	4.93832
202	F	10	S	C(1S)	1.99991	-24.4773		486	N	20	dxz	R(3d)	0.00165	1.95731
203	F	10	S	V(2S)	1.84807	-1.33537		487	N	20	dxz	R(4d)	0.0002	5.15965
204	F	10	S	R(3S)	0.00048	1.53831		488	N	20	dyz	R(3d)	0.00137	1.59797
205	F	10	S	R(4S)	0.00005	2.31215		489	N	20	dyz	R(4d)	0.00006	4.8109
206	F	10	S	R(5S)	0	66.38997		490	N	20	dx2y2	R(3d)	0.00223	1.91646
207	F	10	px	V(2p)	1.91334	-0.4705		491	N	20	dx2y2	R(4d)	0.00016	5.02459
208	F	10	px	R(3p)	0.00109	0.52442		492	N	20	dz2	R(3d)	0.00173	1.90771
209	F	10	px	R(4p)	0.00007	1.79298		493	N	20	dz2	R(4d)	0.00018	5.08955
210	F	10	px	R(5p)	0.00001	5.8738								
211	F	10	py	V(2p)	1.69147	-0.47985		494	C	21	S	C(1S)	1.99923	-10.0818
212	F	10	py	R(3p)	0.0007	0.44373		495	C	21	S	V(2S)	0.82455	-0.10502
213	F	10	py	R(4p)	0.00018	1.91476		496	C	21	S	R(3S)	0.00807	1.00222
214	F	10	py	R(5p)	0.00004	5.84498		497	C	21	S	R(5S)	0.00006	18.60465
215	F	10	pz	V(2p)	1.88982	-0.47034		498	C	21	S	R(4S)	0.00003	3.43767
216	F	10	pz	R(3p)	0.00069	0.46501		499	C	21	px	V(2p)	0.97806	-0.00899
217	F	10	pz	R(4p)	0.00006	1.80075		500	C	21	px	R(4p)	0.01219	1.26921
218	F	10	pz	R(5p)	0.00001	5.79539		501	C	21	px	R(3p)	0.00037	0.53169
219	F	10	dxy	R(3d)	0.00153	2.41528		502	C	21	px	R(5p)	0.00009	2.49102

220	F	10	dxy	R(4d)	0.00001	9.22376		503	C	21	py	V(2p)	0.92767	-0.09716
221	F	10	dxz	R(3d)	0.00056	2.14813		504	C	21	py	R(4p)	0.00062	0.724
222	F	10	dxz	R(4d)	0.00001	9.07828		505	C	21	py	R(3p)	0.00026	0.52799
223	F	10	dyz	R(3d)	0.00164	2.48494		506	C	21	py	R(5p)	0.00005	2.43753
224	F	10	dyz	R(4d)	0.00002	9.25679		507	C	21	pz	V(2p)	0.95488	-0.04913
225	F	10	dx2y2	R(3d)	0.00154	2.47243		508	C	21	pz	R(4p)	0.00717	1.02297
226	F	10	dx2y2	R(4d)	0.00002	9.25168		509	C	21	pz	R(3p)	0.00019	0.64229
227	F	10	dz2	R(3d)	0.00092	2.28071		510	C	21	pz	R(5p)	0.00007	2.49597
228	F	10	dz2	R(4d)	0.00001	9.1537		511	C	21	dxy	R(4d)	0.00062	2.93558
								512	C	21	dxy	R(3d)	0.00003	2.2298
229	F	11	S	C(1S)	1.99991	-24.4775		513	C	21	dxz	R(4d)	0.00054	3.61599
230	F	11	S	V(2S)	1.84849	-1.3354		514	C	21	dxz	R(3d)	0.00004	2.64218
231	F	11	S	R(3S)	0.00048	1.53946		515	C	21	dyz	R(4d)	0.0003	2.87842
232	F	11	S	R(4S)	0.00006	2.299		516	C	21	dyz	R(3d)	0.00008	1.97812
233	F	11	S	R(5S)	0	66.39222		517	C	21	dx2y2	R(4d)	0.00036	3.22514
234	F	11	px	V(2p)	1.90487	-0.47076		518	C	21	dx2y2	R(3d)	0.00004	2.37124
235	F	11	px	R(3p)	0.00109	0.51553		519	C	21	dz2	R(4d)	0.00037	3.04672
236	F	11	px	R(4p)	0.00007	1.8096		520	C	21	dz2	R(3d)	0.00004	2.44989
237	F	11	px	R(5p)	0.00001	5.86626								
238	F	11	py	V(2p)	1.76245	-0.4767		521	N	22	S	C(1S)	1.99958	-14.0583
239	F	11	py	R(3p)	0.00069	0.47222		522	N	22	S	V(2S)	1.59046	-0.57336
240	F	11	py	R(4p)	0.00014	1.87973		523	N	22	S	R(4S)	0.00391	2.2706
241	F	11	py	R(5p)	0.00003	5.82798		524	N	22	S	R(3S)	0.00003	1.03999
242	F	11	pz	V(2p)	1.82786	-0.47312		525	N	22	S	R(5S)	0	35.01531
243	F	11	pz	R(3p)	0.0007	0.44198		526	N	22	px	V(2p)	1.35466	-0.16624
244	F	11	pz	R(4p)	0.00009	1.8489		527	N	22	px	R(3p)	0.00137	0.67782
245	F	11	pz	R(5p)	0.00002	5.79173		528	N	22	px	R(5p)	0.0002	2.81437
246	F	11	dxy	R(3d)	0.00121	2.34016		529	N	22	px	R(4p)	0.00002	2.33259
247	F	11	dxy	R(4d)	0.00001	9.18102		530	N	22	py	V(2p)	1.11135	-0.15067

248	F	11	dxz	R(3d)	0.00093	2.24958		531	N	22	py	R(3p)	0.00061	0.61572
249	F	11	dxz	R(4d)	0.00001	9.13263		532	N	22	py	R(4p)	0.00001	2.23922
250	F	11	dyz	R(3d)	0.00162	2.5451		533	N	22	py	R(5p)	0.00003	2.28564
251	F	11	dyz	R(4d)	0.00002	9.27587		534	N	22	pz	V(2p)	1.2197	-0.15799
252	F	11	dx2y2	R(3d)	0.00119	2.34369		535	N	22	pz	R(3p)	0.00076	0.66624
253	F	11	dx2y2	R(4d)	0.00001	9.19081		536	N	22	pz	R(5p)	0.00006	2.56702
254	F	11	dz2	R(3d)	0.00123	2.32169		537	N	22	pz	R(4p)	0.00002	2.334
255	F	11	dz2	R(4d)	0.00001	9.18337		538	N	22	dxy	R(3d)	0.0033	1.45858
								539	N	22	dxy	R(4d)	0.00004	4.70725
256	F	12	S	C(1S)	1.99992	-24.4751		540	N	22	dxz	R(3d)	0.00642	1.97727
257	F	12	S	V(2S)	1.85261	-1.33246		541	N	22	dxz	R(4d)	0.00003	4.92703
258	F	12	S	R(3S)	0.00049	1.55441		542	N	22	dyz	R(3d)	0.0019	1.36218
259	F	12	S	R(4S)	0.00006	2.29567		543	N	22	dyz	R(4d)	0.00002	4.64054
260	F	12	S	R(5S)	0	66.41975		544	N	22	dx2y2	R(3d)	0.00389	1.64042
261	F	12	px	V(2p)	1.88557	-0.46676		545	N	22	dx2y2	R(4d)	0.00002	4.76944
262	F	12	px	R(3p)	0.00107	0.47882		546	N	22	dz2	R(3d)	0.00318	1.45678
263	F	12	px	R(4p)	0.00005	2.02675		547	N	22	dz2	R(4d)	0.00001	4.72942
264	F	12	px	R(5p)	0.00001	5.65804								
265	F	12	py	V(2p)	1.93338	-0.4646		548	N	23	S	C(1S)	1.9994	-14.1908
266	F	12	py	R(3p)	0.00064	0.48836		549	N	23	S	V(2S)	1.35165	-0.60686
267	F	12	py	R(4p)	0.00003	1.99437		550	N	23	S	R(4S)	0.00039	1.3542
268	F	12	py	R(5p)	0.00001	5.59882		551	N	23	S	R(3S)	0.0001	1.23291
269	F	12	pz	V(2p)	1.67298	-0.47582		552	N	23	S	R(5S)	0	35.24835
270	F	12	pz	R(3p)	0.00074	0.43634		553	N	23	px	V(2p)	1.41679	-0.25607
271	F	12	pz	R(4p)	0.00018	2.14612		554	N	23	px	R(3p)	0.00253	0.66356
272	F	12	pz	R(5p)	0.00004	5.56624		555	N	23	px	R(4p)	0.00011	0.89372
273	F	12	dxy	R(3d)	0.00042	2.12571		556	N	23	px	R(5p)	0.00001	4.38224
274	F	12	dxy	R(4d)	0	9.06833		557	N	23	py	V(2p)	1.67587	-0.27634
275	F	12	dxz	R(3d)	0.00175	2.51147		558	N	23	py	R(3p)	0.00496	0.45801

276	F	12	dxz	R(4d)	0.00002	9.26893		559	N	23	py	R(4p)	0.00011	0.71874
277	F	12	dyz	R(3d)	0.00146	2.3751		560	N	23	py	R(5p)	0.00002	3.9515
278	F	12	dyz	R(4d)	0.00001	9.21498		561	N	23	pz	V(2p)	1.33114	-0.25996
279	F	12	dx2y2	R(3d)	0.0004	2.16373		562	N	23	pz	R(3p)	0.00195	0.62902
280	F	12	dx2y2	R(4d)	0.00001	9.09251		563	N	23	pz	R(4p)	0.00041	0.6374
281	F	12	dz2	R(3d)	0.00211	2.60796		564	N	23	pz	R(5p)	0.00004	4.3956
282	F	12	dz2	R(4d)	0.00003	9.31814		565	N	23	dxy	R(3d)	0.00417	1.47685
								566	N	23	dxy	R(4d)	0.00004	4.93693
								567	N	23	dxz	R(3d)	0.0025	1.63836
								568	N	23	dxz	R(4d)	0.00009	5.0507
								569	N	23	dyz	R(3d)	0.00211	1.32328
								570	N	23	dyz	R(4d)	0.00004	4.86491
								571	N	23	dx2y2	R(3d)	0.00185	1.26835
								572	N	23	dx2y2	R(4d)	0.00003	4.83475
								573	N	23	dz2	R(3d)	0.00246	1.56338
								574	N	23	dz2	R(4d)	0.0001	4.98276
								575	H	24	S	V(1S)	0.61224	0.04357
								576	H	24	S	R(2S)	0.00091	1.16303
								577	H	24	S	R(3S)	0.00028	1.82879
								578	H	24	px	R(2p)	0.00026	2.50633
								579	H	24	py	R(2p)	0.0005	2.25137
								580	H	24	pz	R(2p)	0.00019	2.16766
								581	H	25	S	V(1S)	0.60914	0.0487
								582	H	25	S	R(3S)	0.00046	1.49865
								583	H	25	S	R(2S)	0.00021	1.48888
								584	H	25	px	R(2p)	0.00022	2.5143
								585	H	25	py	R(2p)	0.00044	1.99631

					586	H	25	pz	R(2p)	0.00027	2.41818
--	--	--	--	--	-----	---	----	----	-------	---------	---------

Table S2. Non-bond interactions between carbonitrile and protein.

Favourable non-bond

Distance (Å)	Category	Type	From	From Chemistry	To	To Chemistry
Carbonitrile						
2.10	Hydrogen Bond	Conventional Hydrogen Bond	A:ASP3:HT2	H-Donor	:UNK0:N	H-Acceptor
2.32	Hydrogen Bond;Halogen	Conventional Hydrogen Bond;Halogen (Fluorine)	A:PHE105:HN	H-Donor;Halogen Acceptor	:UNK0:F	H-Acceptor;Halogen
3.03	Hydrogen Bond	Conventional Hydrogen Bond	:UNK0:H	H-Donor	A:PHE105:O	H-Acceptor
2.10	Hydrogen Bond	Conventional Hydrogen Bond	:UNK0:H	H-Donor	A:ILE6:O	H-Acceptor
3.27	Hydrogen Bond;Halogen	Carbon Hydrogen Bond;Halogen (Fluorine)	A:PHE104:CA	H-Donor;Halogen Acceptor	:UNK0:F	H-Acceptor;Halogen
3.00	Hydrogen Bond	Pi-Donor Hydrogen Bond	A:ILE6:HN	H-Donor	:UNK0	Pi-Orbitals
3.52	Halogen	Halogen (Fluorine)	A:LEU103:O	Halogen Acceptor	:UNK0:F	Halogen
Ibuprofen (as reference)						
2.35	Hydrogen Bond	Conventional Hydrogen Bond	A:ARG15:HH21	H-Donor	:UNK0:O	H-Acceptor
2.46	Hydrogen Bond	Conventional Hydrogen Bond	A:GLY18:HN	H-Donor	:UNK0:O	H-Acceptor
2.12	Hydrogen Bond	Conventional Hydrogen Bond	:UNK0:H	H-Donor	A:GLN84:O	H-Acceptor
3.61	Hydrogen Bond	Carbon Hydrogen Bond	A:GLU17:CA	H-Donor	:UNK0:O	H-Acceptor
3.92	Hydrophobic	Pi-Sigma	A:VAL113:CG1	C-H	:UNK0	Pi-Orbitals
Name	Atom	Unsatisfied type		Name	Atom	Unsatisfied type
Carbonitrile						
:UNK0:N	N	Donor	-	-	-	-

:UNK0: carbonitrile; ARG-arginine; ASP-aspartic acid; GLN-glutamine; GLU-glutamic acid; GLY-glycine; ILE-isoleucine; LEU-leucine; PHE-phenylalanine; and VAL-valine